

# MAGNETICALLY DRIVEN WARPING, PRECESSION AND RESONANCES IN ACCRETION DISKS

Dong Lai

Center for Radiophysics and Space Research, Department of Astronomy, Cornell University,  
Ithaca, NY 14853;

E-mail: dong@spacenet.tn.cornell.edu

## ABSTRACT

The inner region of the accretion disk onto a rotating magnetized central star (neutron star, white dwarf or T Tauri star) is subjected to magnetic torques which induce warping and precession of the disk. The origin of these torques lies in the interaction between the surface current on the disk and the horizontal magnetic field (parallel to the disk) produced by the inclined magnetic dipole: The warping torque relies on the radial surface current generated by the twisting of the vertical field threading the disk, while the precessional torque relies on the azimuthal screening current due to the diamagnetic response of the disk. Under quite general conditions, there exists a magnetic warping instability in which the magnetic torque drives the disk plane away from the equatorial plane of the star toward a state where the disk normal vector is perpendicular to the spin axis. Viscous stress tends to suppress the warping instability at large radii, but the magnetic torque always dominates as the disk approaches the magnetosphere boundary. The magnetic torque also drives the tilted inner disk into retrograde precession (opposite to the rotation of the disk) around the stellar spin axis. Moreover, resonant magnetic forcing on the disk can occur which may affect the dynamics of the disk.

The magnetically driven warping instability and precession may be related to a number of observational puzzles. Examples include: (1) Spin evolution of accreting X-ray pulsars: It is suggested that the observed torque reversal of the disk-fed magnetized neutron stars is associated with the wandering of the inner disk around the preferred perpendicular state. (2) Quasi-periodic oscillations in low-mass X-ray binaries: The magnetic torque induces disk tilt, making it possible to explain the observed low-frequency QPOs using disk precession. (3) Super-orbital periods in a number of X-ray binaries as a result of warped, precessing disks. (4) Photometric period variations of T Tauri stars.

*Subject headings:* accretion disks – instabilities – stars: neutron – X-rays: stars – stars: T Tauri – stars: magnetic fields

## 1. INTRODUCTION

Interaction between an accretion disk and a magnetized central object lies at the heart of the physics of a variety of astrophysical systems, including accreting neutron stars, white dwarfs and pre-main-sequence stars (e.g., Frank et al. 1992; Hartmann 1998). The basic picture of disk-magnetosphere interaction was first outlined by Pringle & Rees (1972) following the discovery of accretion-powered X-ray pulsars. These are rotating, highly magnetized ( $B \sim 10^{12}$  G) neutron stars that accrete material from a companion star, either directly from a stellar wind, or in the form of an accretion disk. The strong magnetic field disrupts the accretion flow at the magnetospheric boundary (typically at a few hundreds neutron star radii), and channels the plasma onto the polar caps of the neutron star. The magnetosphere boundary is located where the magnetic and plasma stresses balance,

$$r_m = \eta \left( \frac{\mu^4}{GM\dot{M}^2} \right)^{1/7}, \quad (1-1)$$

where  $M$  and  $\mu$  are the mass and magnetic moment of the central object,  $\dot{M}$  is the mass accretion rate,  $\eta$  is a dimensionless constant of order unity (For an aligned dipole, estimate of  $\eta$  ranges from 0.5 to 1; e.g., Pringle & Rees 1972; Lamb, Pethick & Pines 1973; Ghosh & Lamb 1979a,b, 1992; Aly 1980; Arons 1993; Wang 1995). In low-mass X-ray binaries containing weakly magnetized ( $B \sim 10^8$  G) neutron stars, the magnetosphere lies close to the stellar surface; the neutron stars are spun up and eventually become millisecond pulsars (Alpar et al. 1982; see Phinney & Kulkarni 1994 or Bhattacharya 1995 for a review). Similar magnetosphere-disk interaction also occurs in T Tauri stars (e.g., Hartmann 1998), where the stellar magnetic field ( $B \sim 10^3$  G at the surface) strongly affects the accretion flow, and provides a key ingredient to explain the anomalous slow rotation of these objects (e.g., Königl 1991; Cameron & Campbell 1993; Shu et al. 1994). Finally, models of magnetized accretion disks have been applied to explain the observed UV and X-ray emission from some intermediate polars (the DQ Her subclass of CVs) (e.g., Yi & Kenyon 1997).

A large number of theoretical papers have been written on the subject of the interaction between accretion disk and a magnetized star (e.g., Pringle & Rees 1972; Ghosh & Lamb 1979a,b; Aly 1980; Lipunov & Shakura 1980; Anzer & Börner 1980,1983; Arons 1987,1993; Wang 1987,1995; Aly & Kuijpers 1990; Spruit & Taam 1990,1993; Shu et al. 1994; van Ballegooijen 1994; Lovelace et al. 1995,1998; Li, Wickramasinge & Rüdiger 1996; Campbell 1997), and numerical study of this problem is still in its infancy (e.g., Stone & Norman 1994; Hayashi et al. 1996; Goodson et al. 1997; Miller & Stone 1997; see also Toropin et al. 1999). Beyond the simple notion of magnetosphere (with the Alfvén radius estimated by eq. [1-1]), there is little consensus on the range and strength of magnetic interaction outside the magnetosphere boundary, on the efficiency of magnetic field dissipation in/outside the disk, and on how or where the plasma attaches to the field lines. Outstanding issues include whether the disk excludes the stellar magnetic field by diamagnetic currents or the field can penetrate and thread a large fraction of the disk, whether the threaded field remains closed (connecting the star and the disk) or becomes open by

differential shearing, and whether/how magnetically driven wind is launched from the disk or the magnetosphere/corotation boundary.

This paper introduces some new physical effects associated with disk accretion onto rotating magnetized stars. Most previous papers have, for simplicity, assumed that the stellar magnetic dipole is aligned with the spin axis. Essentially all previous authors, with the exception of Lipunov & Shakura (1980) (see §2.1), have assumed that the spin is aligned with the disk angular momentum — There is a good reason for this, as it is natural to think that the star attains its spin angular momentum from the accretion disk. However, when these assumptions are abandoned, new physical effects are revealed: We show that under quite general conditions, the stellar magnetic field can induce disk warping and make the disk precess around the spin axis. As the accreting plasma approaches the magnetosphere, there is a tendency for the disk plane to be driven away from the equatorial plane of the star toward being aligned with the spin axis (§2 and §4). The origin of the *precessional torque* and *magnetic warping instability* lies in the interaction between the surface current on the disk and the horizontal magnetic field (parallel to the disk) produced by the stellar dipole. The electric current on the disk is an inevitable consequence of magnetic-field – disk interaction, although its actual form is uncertain and depends on whether the disk is diamagnetic or has a vertical field threading it, thus on the dissipative processes in the disk and the magnetosphere (§2). The magnetic force on the disk also give rise to vertical and epicyclic resonances which may drive disk perturbations (§3). We show that the magnetically driven warping and precession of accretion disks can potentially explain a number of outstanding puzzles related to disk accretion onto magnetized stars (§6).

This paper is organized as follows. In §2 we calculate the precessional and warping torques on the disk (or a ring of disk) due to the stellar magnetic field for several models based on different assumptions about magnetic field – disk interaction. The torques are different for different models, but they are always present and are of the same order of magnitude. The key physics of the torques are summarized at the beginning of §2. Resonances due to magnetic forces on the disk are discussed in §3. In §4 we study the dynamics of a warped disk under the influence of the magnetic torques derived in §2. The criterion for the magnetically driven warping instability (including the effect of viscosity) is derived, and a magnetic “Bardeen-Petterson” effect is discussed. Section 5 addresses the question of how the spin of the central star is affected by the warped, precessing disk. In §6 we discuss/speculate several astrophysical applications of our theory, including the spin evolution of accretion-powered X-ray pulsars, quasi-periodic oscillations in low-mass X-ray binaries, long-term periodic cycles in several X-ray binaries, and the variability and rotation of T Tauri stars. We conclude in §7 by discussing possible future studies along the line initiated in this paper.

Because of the intrinsic uncertainties associated with the nature of magnetic field – disk interaction, in the main text we shall focus on generic features and rely on parametrized models. In Appendix A we discuss a global magnetized disk model. In Appendix B we consider the issue of calculating the magnetosphere radius for nontrivial magnetic field and spin geometry. The

dynamics of an extreme form of disk (consisting of diamagnetic blobs) is examined in Appendix C.

## 2. MAGNETIC PRECESSIONAL AND WARPING TORQUES

In this section we calculate the magnetic torque on the disk (or a ring of disk) surrounding a rotating magnetic dipole. Because of the uncertainties on how the magnetic field behaves in the presence of an accretion disk (see §1), we shall consider several different models, some representing extreme situations. Our most “realistic” model is given in §2.3.

The basic set-up used in our calculation is shown in Fig. 1. The disk angular momentum axis  $\hat{l}$  is inclined by an angle  $\beta$  with respect to the spin axis  $\hat{\omega}$ . The stellar dipole moment  $\hat{\mu}$  rotates around the spin axis  $\hat{\omega}$ . The angle of obliquity between the magnetic moment and the rotation axis is  $\theta$ .

The key physics responsible for the magnetic torques on the disk is as follows:

(i) If the disk is diamagnetic (perfectly conducting) so that the vertical stellar field (perpendicular to the disk) cannot penetrate, an azimuthal screening surface current will be induced in the disk. This current interacts with the radial magnetic field from the star, and a vertical magnetic force results. While the mean force (averaging over the azimuthal) is zero, the uneven distribution of the force induces a net torque acting on the ring, making it precess around the spin axis. (For a nonrotating star, the disk will precess around the magnetic axis.) (§2.1).

(ii) If there is a vertical field threading the disk (this  $B_z$  either comes from the star or is carried intrinsically by the disk and detached from the star), it will be twisted by the disk rotation to produce a discontinuous azimuthal field  $\Delta B_\phi$  across the disk surface, and a radial surface current results. The interaction between this current and the stellar  $B_\phi$  (which is not affected by the disk) gives rise to a vertical force, and the resulting torque tends to misalign the angular momentum of the ring with the spin axis (although in some extreme situations, alignment torque may also result). (For a nonrotating star, the disk normal will be driven away from the stellar magnetic axis.) (§2.2).

In general, we expect both types of torques to exist on the disk (§2.3 and §2.4).

### 2.1. Diamagnetic Disk

Here we consider the extreme situation where the disk is a perfect conductor and has no large-scale magnetic field of its own. The inner radius of the disk is located at  $r = r_m$ , the magnetospheric radius. The magnetic field produced by the stellar dipole cannot penetrate the disk, and a diamagnetic surface current is induced. Aly (1980) has found the exact analytic solution to this model problem (see also Kundt & Robnik 1980; Riffert 1980). The magnetic field

at a point  $(r, \phi, z = 0)$  (cylindrical coordinates) on the disk surface ( $z = 0, r > r_m$ ) is given by

$$B_r = \frac{2\mu}{r^3} \sin \chi \cos(\phi - \phi_\mu) \mp \frac{4\mu}{\pi r^3 D} \cos \chi, \quad (2-1)$$

$$B_\phi = \frac{\mu}{r^3} \sin \chi \sin(\phi - \phi_\mu), \quad (2-2)$$

$$B_z = 0, \quad (2-3)$$

where  $\chi$  and  $\phi_\mu$  are defined in Fig. 1 (they are both varying in time). In eq. (2-1), the upper (lower) sign applies to the upper (lower) disk surface, and the factor  $D$  is

$$D = \max \left( \sqrt{r^2/r_m^2 - 1}, \sqrt{2H/r_m} \right), \quad (2-4)$$

(where  $H \ll r_m$  is the half-thickness of the disk). The discontinuity in  $B_r$  implies a surface current

$$\mathbf{K} = -\frac{2c\mu}{\pi^2 r^3 D} \cos \chi \hat{\phi} \quad (2-5)$$

( $\hat{\phi}$  is the unit vector along the  $\phi$  direction; similar notation will be used throughout the paper). Note that this surface current is induced to cancel the  $z$ -component of the stellar field,  $B_z^{(0)} = -\mu \cos \chi / r^3$ ; the  $r, \phi$ -components of the stellar field [the first terms of eqs. (2-1) and (2-2)] do not induce any net surface current. (In fact, they induce currents on the upper and lower surfaces of the disk, but these currents have opposite directions. Such currents can lead to the “squeezing” of the disk — changing the thickness of the disk, but not the “lifting”.) The magnetic force per unit area on the disk results from the interaction between  $\mathbf{K}$  and  $B_r^{(0)}$  (the first term in eq. [2-1]):

$$\mathbf{F} = \frac{2\mu^2}{\pi^2 r^6 D} \sin 2\chi \cos(\phi - \phi_\mu) \hat{z}. \quad (2-6)$$

The existence of this vertical magnetic force has already been noted by Aly (1980), and it is simply the difference in the magnetic pressure,  $B^2/(8\pi)$ , between the lower and upper surfaces. The magnetic torque per unit area is

$$\mathbf{N} = \mathbf{r} \times \mathbf{F} = -\frac{2\mu^2}{\pi^2 r^5 D} \sin 2\chi \cos(\phi - \phi_\mu) \hat{\phi}. \quad (2-7)$$

Clearly, averaging the force over the azimuthal angle,  $\langle \mathbf{F} \rangle_\phi = (1/2\pi) \int_0^{2\pi} d\phi \mathbf{F}$ , gives zero, but the azimuthally averaged torque is nonzero, and given by

$$\langle \mathbf{N} \rangle_\phi = \frac{\mu^2}{\pi^2 r^5 D} \sin 2\chi (\sin \phi_\mu \hat{x} - \cos \phi_\mu \hat{y}) = \frac{2\mu^2}{\pi^2 r^5 D} \cos \chi (\hat{\mu} \times \hat{l}), \quad (2-8)$$

( $\hat{\mu}$  and  $\hat{l}$  are the unit vectors along the dipole moment and the disk angular momentum, respectively). For nonrotating star, this result implies that the magnetic torque tends to make the disk precess around the magnetic axis  $\hat{\mu}$ . For a rotating star — as long as the rotation period is

much shorter than the precession period, we need to average over the spin period. The following identities will be needed:

$$\cos \chi = \cos \beta \cos \theta - \sin \beta \sin \theta \sin \omega t, \quad (2-9)$$

$$\sin \chi \cos \phi_\mu = \sin \theta \cos \omega t, \quad (2-10)$$

$$\sin \chi \sin \phi_\mu = \sin \beta \cos \theta + \cos \beta \sin \theta \sin \omega t, \quad (2-11)$$

where an appropriate phase for the stellar rotation has been adopted. We find that, after averaging over the spin period, the torque per unit area  $\langle\langle \mathbf{N} \rangle\rangle \equiv \langle\langle \mathbf{N} \rangle_\phi \rangle_\omega \equiv (1/P_s) \int_0^{P_s} dt \langle \mathbf{N} \rangle_\phi$  (where  $P_s = 2\pi/\omega$  is the spin period) is given by

$$\langle\langle \mathbf{N} \rangle\rangle = \frac{\mu^2}{\pi^2 r^5 D} \cos \beta \left( 3 \cos^2 \theta - 1 \right) (\hat{\omega} \times \hat{l}). \quad (2-12)$$

The magnetic torque on a ring of radius  $r$  and width  $dr$  is simply  $d\mathbf{T} = 2\pi r \langle\langle \mathbf{N} \rangle\rangle dr$ . The angular momentum of the ring is  $(2\pi r \Sigma dr)(r^2 \Omega)$  (where  $\Sigma$  is the surface density of the disk, and  $\Omega$  is the orbital angular frequency). Thus the effect of the magnetic torque is to make the ring precess around the spin axis  $\hat{\omega}$  at an angular frequency

$$\mathbf{\Omega}_{\text{prec}} = \frac{\mu^2}{\pi^2 r^7 \Omega \Sigma D} \cos \beta \left( 3 \cos^2 \theta - 1 \right) \hat{\omega}. \quad (2-13)$$

Note that the sign of  $\cos \beta (3 \cos^2 \theta - 1)$  determines whether  $\mathbf{\Omega}_{\text{prec}}$  is along  $\hat{\omega}$  or opposite to it. This result has been obtained previously by Lipunov & Shakura (1980)<sup>1</sup>.

## 2.2. Magnetically Threaded Disk

We now consider the opposite limit in which the stellar magnetic field rapidly penetrates the disk (on a timescale shorter than the dynamical time of the disk) (see §2.3). Because of the shear between the disk and the plasma outside the disk, the threaded vertical field is winded to produce an azimuthal field which has different signs on the upper and lower surfaces of the disk. We thus

---

<sup>1</sup>Lipunov & Shakura (1980) also argued that for  $\cos^2 \theta < 1/3$ , the minimum of the interaction energy between the central dipole and the field generated by the disk current is achieved at  $\beta = 0^\circ$ , while for  $\cos^2 \theta > 1/3$ , the minimum energy corresponds to  $\beta = 90^\circ$ . They therefore suggested that in the latter case ( $\cos^2 \theta > 1/3$ ), the disk tends to evolve into the  $\beta = 90^\circ$  state. However, if eq. (2-12) is the only torque present in the disk, it is not clear how  $\beta$  can change. Moreover, the “magnetic Bardeen-Petterson” effect always tends to align  $\hat{l}$  and  $\hat{\omega}$ , independent of the sign of  $\mathbf{\Omega}_{\text{prec}}$  (see §4.2). I became aware of the papers by Lipunov et al. (see also Lipunov, Semënov & Shakura 1981) in mid-February 1999, at which point this paper was nearly finished. For completeness and pedagogical reason, I have decided to keep this subsection (§2.1) in its original form. I thank Dr. Brad Hansen (CITA) for drawing my attention to the papers by Lipunov et al.

adopt the following *ansatz* for the magnetic field in the disk<sup>2</sup>:

$$B_r = \frac{2\mu}{r^3} \sin \chi \cos(\phi - \phi_\mu), \quad (2-14)$$

$$B_\phi = \frac{\mu}{r^3} \sin \chi \sin(\phi - \phi_\mu) \pm \zeta \frac{\mu}{r^3} \cos \chi, \quad (2-15)$$

$$B_z = -\frac{\mu}{r^3} \cos \chi. \quad (2-16)$$

In (2-15), the second term represents the field produced by the twisting of  $B_z$ , and the upper (lower) sign corresponds to the value at the upper (lower) disk surface<sup>3</sup>. The quantity  $\zeta$  specifies the azimuthal pitch of the field line. In general we expect  $|\zeta| \lesssim 1$  (e.g., Sturrock & Barnes 1972; Lovelace et al. 1995 and references therein), but its actual value or form depends on details of the dissipative processes involved in the disk-magnetic field interactions. If the stellar magnetic field threads the disk in a closed configuration (e.g., Ghosh & Lamb 1979a,b; Wang 1987,1995), we expect  $\zeta \propto (\Omega - \omega)$  so that  $\zeta > 0$  for  $\Omega > \omega$  and  $\zeta < 0$  for  $\Omega < \omega$ . But it has been argued that the differential shearing and the plasma flowing from the disk into the overlying magnetosphere will blow the field lines open and maintain them in an open configuration (e.g., Arons 1987; Newman et al. 1992; Lynden-Bell & Boily 1994; Lovelace et al. 1995 and references therein), in which case we expect  $\zeta$  to be positive and of order unity. For our purpose in this paper,  $\zeta$  is simply a dimensionless number or function<sup>4</sup>. Also note that because of the screening currents in the disk (such as those discussed in §2.1) or in the magnetosphere boundary, the threaded field may be smaller than the vacuum field produced by the dipole. But since our result (see below) depends on  $\zeta\mu^2$ , we can easily absorb the screening effect into the definition of  $\zeta$ .

---

<sup>2</sup> In principle, an additional radial field  $\Delta B_r$  could be generated (with opposite signs in the upper and lower disk surfaces) when the radial inflow of the disk drags the threaded  $B_z$ . This discontinuous  $\Delta B_r$  will give rise to a precessional torque similar to that derived in §2.1. Since we expect  $\Delta B_r$  to be proportional to the radial velocity, it is neglected in eq. (2-14).

<sup>3</sup> There could be an additional contribution to  $B_\phi$  on the right-hand side of (2-15) due to the shearing of the stellar  $B_r$  by the differential rotation. This contribution is not included for two reasons. First, the stellar  $B_r$  may not be able to penetrate the thin disk; Second, even if a component of  $B_r$  (e.g., the static component; see §2.3) penetrates the disk, the induced  $\Delta B_\phi$  is expected to be smaller than that due to the threaded  $B_z$ . To see this, we write, schematically,

$$\frac{\partial \Delta B_\phi}{\partial t} = r \left( B_z \frac{\partial \Omega}{\partial z} + B_r \frac{\partial \Omega}{\partial r} \right) - \frac{\Delta B_\phi}{\tau_{\text{diss}}},$$

where  $B_z$  and  $B_r$  are the threaded fields,  $\tau_{\text{diss}}$  is the effective dissipation time. In steady state, we find

$$\Delta B_\phi = \mp \zeta B_z - \frac{3}{2} \tau_{\text{diss}} \Omega B_r,$$

where  $\zeta = (r/H_B)\tau_{\text{diss}}(\Omega - \omega)$  (for closed field configurations) or  $\zeta = (r/H_B)\tau_{\text{diss}}\Omega$  (for open field configurations) ( $H_B$  is the vertical scale in which  $\Omega$  varies). Note that the shearing of  $B_r$  does not produce any surface current. For  $H_B \ll r$ , we can drop the term proportional  $B_r$  in  $\Delta B_\phi$ , and obtain  $\Delta B_\phi = \mp \zeta B_z$ .

<sup>4</sup>Even in models (e.g., Shu et al. 1994) where the disk is largely diamagnetic with no intrinsic  $B_z$ , the stellar field must penetrate the boundary layer. In this case, one would imagine that  $\zeta$  is nonzero only near the magnetosphere boundary.

The surface current on the disk corresponding to the field (2-14)-(2-16) is

$$\mathbf{K} = -\frac{\zeta c \mu}{2\pi r^3} \cos \chi \hat{r}. \quad (2-17)$$

The interaction of  $\mathbf{K}$  with  $B_z$  gives rise to an azimuthal force, which tends to slow down (or speed up if  $\omega > \Omega$  and the field lines are in a closed configuration) the fluid motion, transferring angular momentum between the disk and the overlying magnetosphere or the star. This is the familiar magnetic braking torque which has been included in previous studies of aligned magnetized disk (e.g., Ghosh & Lamb 1979a,b; Lovelace et al. 1995; Wang 1995; Lai 1998). Here we are interested in the vertical magnetic force  $F_z$  (per unit area), resulting from the interaction between  $\mathbf{K}$  and the azimuthal field produced by the stellar dipole (the first term in [2-15]):

$$F_z = -\frac{\zeta \mu^2}{4\pi r^6} \sin 2\chi \sin(\phi - \phi_\mu). \quad (2-18)$$

This is simply the difference in  $B^2/(8\pi)$  below and above the disk. The magnetic torque associated with  $F_z$  is given by

$$\mathbf{N} = \frac{\zeta \mu^2}{4\pi r^5} \sin 2\chi \sin(\phi - \phi_\mu) \hat{\phi}. \quad (2-19)$$

Averaging over  $\phi$ , we have

$$\langle \mathbf{N} \rangle_\phi = -\frac{\zeta \mu^2}{8\pi r^5} \sin 2\chi (\cos \phi_\mu \hat{x} + \sin \phi_\mu \hat{y}) = -\frac{\zeta \mu^2}{4\pi r^5} (\hat{l} \cdot \hat{\mu}) [\hat{\mu} - (\hat{\mu} \cdot \hat{l}) \hat{l}]. \quad (2-20)$$

For a nonrotating star, this torque tends to pull the disk normal vector  $\hat{l}$  toward being perpendicular to the magnetic axis  $\hat{\mu}$  (assuming  $\zeta > 0$ ), thus making the disk plane parallel to the stellar field lines. For a rotating star, averaging over the spin period and using the identities (2-9)-(2-11), we find

$$\begin{aligned} \langle \langle \mathbf{N} \rangle \rangle &= -\frac{\zeta \mu^2}{16\pi r^5} \sin 2\beta (3 \cos^2 \theta - 1) \hat{y} \\ &= -\frac{\zeta \mu^2}{8\pi r^5} \cos \beta (3 \cos^2 \theta - 1) [\hat{\omega} - (\hat{\omega} \cdot \hat{l}) \hat{l}]. \end{aligned} \quad (2-21)$$

In the absence of other forces, this magnetic torque will change the tilt angle  $\beta$  of the ring (at radius  $r$ ) according to

$$\frac{d\beta}{dt} = \frac{\zeta \mu^2}{16\pi r^7 \Omega \Sigma} \sin 2\beta (3 \cos^2 \theta - 1). \quad (2-22)$$

Thus, depending on the sign of  $\zeta \cos \beta (3 \cos^2 \theta - 1)$ , the angle  $\beta$  can increase or decrease: For  $\zeta (3 \cos^2 \theta - 1) > 0$ , the torque drives the disk toward the perpendicular configuration ( $\beta = 90^\circ$ ), while for  $\zeta (3 \cos^2 \theta - 1) < 0$ , it drives the disk toward alignment ( $\beta = 0^\circ$ ) or anti-alignment ( $\beta = 180^\circ$ ). In particular, when  $\zeta (3 \cos^2 \theta - 1) > 0$ , the aligned configuration is unstable against the growth of disk tilt angle — This is the *magnetic warping instability* (see §2.3 and §2.4).

It is instructive to understand the difference between the situation studied here and that of a diamagnetic disk considered in §2.1. In both cases, a vertical magnetic force is exerted on the disk.



Although eqs. (2-6) and (2-18) appear similar, they have very different spin-averaged behavior. For a diamagnetic disk, we have

$$\langle F_z \rangle_\omega = \frac{\mu^2}{\pi^2 r^6 D} \sin 2\beta \left( 3 \cos^2 \theta - 1 \right) \sin \phi. \quad (2-23)$$

Thus the force on the  $y > 0$  side of the disk has a different sign from that on the  $y < 0$  side, giving rise to a torque which is along the  $x$ -axis (perpendicular to both  $\hat{l}$  and  $\hat{\omega}$ ). For a magnetically threaded disk, we have

$$\langle F_z \rangle_\omega = \frac{\zeta \mu^2}{8\pi r^6} \sin 2\beta \left( 3 \cos^2 \theta - 1 \right) \cos \phi. \quad (2-24)$$

The force has different signs for  $x > 0$  and  $x < 0$ , and the torque is along the  $y$ -axis (in the same plane as  $\hat{l}$  and  $\hat{\omega}$ ).

### 2.3. A Hybrid “Realistic” Model

The results of §2.1 and §2.2 represent two opposite, extreme situations, and are not likely to be realistic. The magnetic field configuration in a purely diamagnetic disk (see §2.1) is prone to Kelvin-Helmholtz instability and reconnection. It has been argued that the non-linear development of these processes could lead to partial threading of the magnetic field through the disk (e.g., Ghosh & Lamb 1979a,b; Wang 1987, 1995), although the extent of the field-threading region is uncertain and the closed configuration advocated by Ghosh and Lamb is probably unrealistic (e.g., Arons 1987; Shu et al. 1994; Lovelace et al. 1995). In any event, near the magnetosphere boundary, the vertical stellar field must certainly thread the disk plasma. On the other hand, the magnetically threaded disk model considered in §2.2 requires that the stellar field penetrates the disk almost instantaneously (compared to the spin period and the orbital period). This is unrealistic. The timescale for field penetration is uncertain, but it cannot be shorter than the dynamical time of the disk; it may be as long as the disk thermal time (E. T. Vishniac 1999, private communication; see Park & Vishniac 1996 and references therein).

The vertical vacuum field produced by the stellar dipole on the disk can be written as the sum of a static component and a time-varying component:

$$B_z^{(0)} = -\frac{\mu}{r^3} \cos \chi = -\frac{\mu}{r^3} \cos \beta \cos \theta + \frac{\mu}{r^3} \sin \beta \sin \theta \sin \omega t. \quad (2-25)$$

While it is possible that the static field can penetrate the disk by allowing sufficient time for Kelvin-Helmholtz instability/reconnection to grow, it is almost certain that the variable field will be shielded out of the disk by the screening current. We therefore consider the following hybrid model, which we consider to be more realistic than the situations studied in §2.1 and §2.2: The static component of the vertical stellar field threads the disk, while the time-varying component is screened out by the disk. The winding of the threaded field will produce an azimuthal field and a radial surface current, while the variable vertical field will induce a shielding azimuthal

surface current and discontinuous radial field — this radial field can be obtained by appropriately modifying Aly’s solution as given in §2. The magnetic field on the disk is then given by <sup>5</sup>

$$B_r = \frac{2\mu}{r^3} \sin \chi \cos(\phi - \phi_\mu) \pm \frac{4\mu}{\pi r^3 D} \sin \beta \sin \theta \sin \omega t, \quad (2-26)$$

$$B_\phi = \frac{\mu}{r^3} \sin \chi \sin(\phi - \phi_\mu) \pm \zeta \frac{\mu}{r^3} \cos \beta \cos \theta, \quad (2-27)$$

$$B_z = -\frac{\mu}{r^3} \cos \beta \cos \theta. \quad (2-28)$$

In (2-26),  $B_r$  is the sum of the vacuum dipole field and the field produced by the azimuthal screening current (which is induced to cancel the variable part of  $B_z^{(0)}$ ); in (2-27),  $B_\phi$  is the sum of the vacuum dipole field and the field induced by the winding of the constant  $B_z$  (see §2.2 for the property of  $\zeta$ ). The surface current on the disk is

$$\mathbf{K} = \frac{2c\mu}{\pi^2 r^3 D} \sin \beta \sin \theta \sin \omega t \hat{\phi} - \frac{\zeta c\mu}{2\pi r^3} \cos \beta \cos \theta \hat{r}. \quad (2-29)$$

The vertical magnetic force (per unit area) on the disk is then given by

$$F_z = -\frac{4\mu^2}{\pi^2 r^6 D} \sin \beta \sin \theta \sin \omega t \sin \chi \cos(\phi - \phi_\mu) - \frac{\zeta\mu^2}{2\pi r^6} \cos \beta \cos \theta \sin \chi \sin(\phi - \phi_\mu). \quad (2-30)$$

The corresponding torque (per unit area) acting on the disk, averaged over the ring, is given by

$$\langle \mathbf{N} \rangle_\phi = -\frac{2\mu^2}{\pi^2 r^5 D} \sin \beta \sin \theta \sin \omega t (\hat{\mu} \times \hat{l}) - \frac{\zeta\mu^2}{4\pi r^5} \cos \beta \cos \theta [\hat{\mu} - (\hat{\mu} \cdot \hat{l})\hat{l}]. \quad (2-31)$$

For nonrotating star, eq. (2-31) reduces to eq. (2-20) (note that  $\cos \chi = \cos \beta \cos \theta$  when  $\omega = 0$ ): The torque tends to make the disk plane align with the stellar field lines (i.e.,  $\hat{l}$  perpendicular to  $\hat{\mu}$ ). Averaged over the stellar rotation, the torque can be written as

$$\langle \langle \mathbf{N} \rangle \rangle = \langle \langle \mathbf{N} \rangle \rangle_{\text{prec}} + \langle \langle \mathbf{N} \rangle \rangle_{\text{warp}}, \quad (2-32)$$

where the precessional torque and the warping torque are given by

$$\langle \langle \mathbf{N} \rangle \rangle_{\text{prec}} = -\frac{\mu^2}{\pi^2 r^5 D} \cos \beta \sin^2 \theta (\hat{\omega} \times \hat{l}), \quad (2-33)$$

$$\langle \langle \mathbf{N} \rangle \rangle_{\text{warp}} = -\frac{\zeta\mu^2}{8\pi r^5} \sin 2\beta \cos^2 \theta \hat{y} = -\frac{\zeta\mu^2}{4\pi r^5} \cos \beta \cos^2 \theta [\hat{\omega} - (\hat{\omega} \cdot \hat{l})\hat{l}]. \quad (2-34)$$

Clearly, the diamagnetic feature of the disk induces a precessional torque (eq. [2-33]), with the precession angular frequency given by

$$\Omega_{\text{prec}} = -\frac{\mu^2}{\pi^2 r^7 \Omega \Sigma D} \cos \beta \sin^2 \theta \hat{\omega}. \quad (2-35)$$

---

<sup>5</sup>In eq. (2-26) we have neglected a possible component of  $B_r$  generated by radial infall of the threaded  $B_z$ ; See footnote 2. Also, in (2-27) we have ignored a possible toroidal field generated by the shearing of the stellar  $B_r$ ; see footnote 3.

On the other hand, the disk-threading field gives rise to a torque (eq. [2-34]) which changes  $\beta$  at a rate given by

$$\frac{d\beta}{dt} = \frac{\zeta\mu^2}{8\pi r^7 \Omega \Sigma} \sin 2\beta \cos^2 \theta. \quad (2-36)$$

Note that the disk precession is along the direction  $(-\cos\beta\hat{\omega})$ , i.e., the precession is always in the opposite sense as the orbital motion of disk. Equation (2-36) reveals the *magnetic warping instability*: the spin-orbit inclination angle  $\beta$  increases when  $\zeta \cos\beta > 0$  and decreases when  $\zeta \cos\beta < 0$ . Thus, for  $\zeta > 0$  (the most likely case; see §2.2), the warping torque always tends to drive the disk toward the configuration where  $\hat{l}$  is perpendicular to  $\hat{\omega}$ .

## 2.4. General Consideration

The preceding subsections assume that the vertical field that threads the disk originates from the star. But it is important to note that this is not a requirement for the existence of the warping torque. Indeed, models of hydromagnetic driven outflows from disks are predicated on the existence of large-scale poloidal magnetic field that threads the disk — this field could have been advected inward by the accreting flow or generated in the disk (see, e.g., Blandford 1989 for a review).

Suppose there is vertical  $B_z$  (assumed to be time-independent) which threads the disk. The warping torque results from the interaction of the stellar  $B_\phi$  and the radial surface current on the disk induced by the twisting of the threaded  $B_z$ . Thus in general, we can write the azimuthal field on the disk as

$$B_\phi = \frac{\mu}{r^3} \sin\chi \sin(\phi - \phi_\mu) \mp \zeta B_z, \quad (2-37)$$

with  $\zeta$  a positive dimensionless number of order or less than unity. The vertical force on the disk is given by

$$F_z = \frac{\zeta\mu B_z}{2\pi r^3} \sin\chi \sin(\phi - \phi_\mu). \quad (2-38)$$

The averaged (warping) torque is then

$$\langle\langle \mathbf{N} \rangle\rangle = \frac{\zeta\mu B_z}{4\pi r^2} \sin\beta \cos\theta \hat{y}. \quad (2-39)$$

The model considered in §2.3 corresponds to  $B_z = -\mu \cos\beta \cos\theta/r^3$ .

The precessional torque results from the interaction of the ring of diamagnetic screening current and the radial magnetic field produced by the star. Assume that the surface current has the form

$$\mathbf{K} = (K_{\phi 1} + K_{\phi 2} \sin\omega t) \hat{\phi}. \quad (2-40)$$

(In general, both the static current  $K_{\phi 1}$  and the time-dependent current  $K_{\phi 2} \sin\omega t$  are possible as the disk responds to the external field that tries to enter the disk.) The vertical magnetic force is

$$F_z = -\frac{2\mu}{cr^3} (K_{\phi 1} + K_{\phi 2} \sin\omega t) \sin\chi \cos(\phi - \phi_\mu), \quad (2-41)$$

and the resulting averaged (precessional) torque is

$$\langle\langle\mathbf{N}\rangle\rangle = -\frac{\mu}{cr^2} \left( K_{\phi 1} \sin \beta \cos \theta + \frac{K_{\phi 2}}{2} \cos \beta \sin \theta \right) \hat{x}. \quad (2-42)$$

The model considered in §2.3 corresponds to  $K_{\phi 1} = 0$  and  $K_{\phi 2} = (2c\mu/\pi^2 r^3 D) \sin \beta \sin \theta$ , while in the model considered in §2.1, we have  $K_{\phi 1} = -(2c\mu/\pi^2 r^3 D) \cos \beta \cos \theta$  and  $K_{\phi 2} = (2c\mu/\pi^2 r^3 D) \sin \beta \sin \theta$ .

Finally, we note that in our calculations of the warping torques (§2.2-§2.4) we have assumed that the azimuthal pitch  $\zeta$  is stationary in time. An alternative scenario has been proposed (Aly & Kuipers 1990; van Ballegoijen 1994), where the threaded field lines are being constantly wound up, with occasional field reconnection which releases the stored-up magnetic energy. Even for such a time-dependent magnetic field structure (apart from the time-dependence of the rotating dipole field), it is likely that magnetic torques (similar to those calculated in this paper) will exist, although this possible complication will be ignored in this paper.

### 2.5. Disk Consisting of Diamagnetic Blobs

The previous subsections treat the disk as a continuum. It has been suggested that under certain conditions, the accretion disk may be lumpy, consisting of diamagnetic blobs (Vietri & Stella 1998; see King 1993). Such inhomogeneous accretion flow may arise from the nonlinear development of various plasma instabilities (e.g., Kelvin-Helmholtz instability; Arons & Lea 1980) associated with the disk and the magnetosphere. Vietri & Stella (1998) studied the motion of diamagnetic blobs orbiting a central star with an inclined magnetic dipole and showed that magnetic drag force (Drell, Foley & Ruderman 1965) on the blob can induce vertical resonances near the corotation radius of the disk.

We have calculated the magnetic torque on the accretion disk consisting of individual diamagnetic blobs. It can be shown that independent of the vertical resonances, there exists a magnetic torque which tends to induce tilt on the orbit of the blob. Since there are considerable uncertainties associated with such an extreme form of accretion disk, we relegate the calculation to Appendix C.

## 3. MAGNETICALLY DRIVEN RESONANCES

The discussion in §2 has neglected possible resonances in the interaction between the disk the rotating central dipole. Here we consider these resonances.

### 3.1. Vertical and Epicyclic Resonances

The bending mode of the disk is characterized by a small vertical displacement  $Z(r, \phi, t)$ , with the equation of motion

$$\frac{d^2 Z}{dt^2} = \left( \frac{\partial}{\partial t} + \Omega \frac{\partial}{\partial \phi} \right)^2 Z = -\Omega_z^2 Z + \frac{1}{\Sigma} F_z, \quad (3-1)$$

where  $\Omega$  is the orbital angular frequency, the term  $-\Omega_z^2 Z$  represents vertical the gravitational restoring force (for a Keplerian disk,  $\Omega_z = \Omega$ ), and  $F_z$  is the magnetic force (per unit area) as calculated in §2. Pressure, viscous force and self-gravity have been neglected.

Consider first the magnetic force given by eq. (2-38), and write it as

$$F_z = \frac{\zeta \mu B_z}{2\pi r^3} \left[ \sin \theta \cos \omega t \sin \phi - (\sin \beta \cos \theta + \cos \beta \sin \theta \sin \omega t) \cos \phi \right]. \quad (3-2)$$

There exists the following possible vertical resonances:

$$\Omega_z = \Omega \quad (\text{for } \sin \beta \cos \theta \neq 0) \quad (3-3)$$

$$\omega - \Omega = \pm \Omega_z \quad (\text{for } \sin \theta \neq 0 \text{ and } \beta \neq \pi) \quad (3-4)$$

$$\omega + \Omega = \Omega_z \quad (\text{for } \sin \theta \neq 0 \text{ and } \beta \neq 0). \quad (3-5)$$

These resonances can be easily understood: (1) When  $\sin \beta \cos \theta \neq 0$ , there exists a static distribution ( $\propto \cos \phi$ ) of vertical force field, and a fluid element feels the force  $\propto \cos \Omega t$ ; this explains the  $\Omega = \Omega_z$  resonance. (2) When  $\sin \theta \neq 0$ , there exists a time-dependent vertical force field ( $\propto \sin \omega t$  or  $\cos \omega t$ ). A fluid element, traveling with angular velocity  $\Omega$ , would experience vertical forces with frequency  $(\omega \pm \Omega)$  [for  $\beta = 0$ , only  $(\omega - \Omega)$  is possible, while for  $\beta = 180^\circ$ , only  $(\omega + \Omega)$  is possible]; this explains the  $\omega \pm \Omega = \pm \Omega_z$  resonances.

Now consider the magnetic force given by eq. (2-41). The force associated with  $K_{\phi 1}$  has the form  $\sin \phi$  and  $\cos(\phi \pm \omega t)$ , which would give rise to the  $\Omega_z = \Omega$  resonance and the  $\omega \pm \Omega = \pm \Omega_z$  resonances as in eqs. (3-3)-(3-5). The force associated with  $K_{\phi 2}$  has a time-dependence of the form

$$\begin{aligned} \sin \omega t \sin \chi \cos(\phi - \phi_\mu) &= \frac{1}{2} \cos \beta \sin \theta \sin \phi + \sin \beta \cos \theta \sin \omega t \sin \phi \\ &\quad + \frac{1}{2} \sin \theta \left( \sin 2\omega t \cos \phi - \cos \beta \cos 2\omega t \sin \phi \right). \end{aligned} \quad (3-6)$$

This gives rise to the following resonances:

$$\Omega_z = \Omega \quad (\text{for } \cos \beta \sin \theta \neq 0) \quad (3-7)$$

$$\omega \pm \Omega = \pm \Omega_z \quad (\text{for } \sin \beta \cos \theta \neq 0) \quad (3-8)$$

$$2\omega - \Omega = \pm \Omega_z \quad (\text{for } \sin \theta \neq 0 \text{ and } \beta \neq \pi) \quad (3-9)$$

$$2\omega + \Omega = \Omega_z \quad (\text{for } \sin \theta \neq 0 \text{ and } \beta \neq 0). \quad (3-10)$$

The new resonances,  $2\omega \pm \Omega = \pm \Omega_z$ , come about because the magnetic field varies as  $\cos \omega t$  or  $\sin \omega t$ , and the screening current also varies as  $\cos \omega t$  or  $\sin \omega t$ .

In addition to the vertical resonances discussed above, epicyclic resonance can also arise from the magnetic field – disk interaction. Consider the field given by eqs. (2-26)-(2-28). The interaction between  $K_\phi$  with  $B_z$  gives rise to a radial force

$$F_r = -\frac{\mu^2}{2\pi^2 r^6 D} \sin 2\beta \sin 2\theta \sin \omega t. \quad (3-11)$$

Clearly, epicyclic resonance occurs when

$$\kappa = \omega \quad (\text{for } \sin 2\beta \sin 2\theta \neq 0), \quad (3-12)$$

where  $\kappa$  is the epicyclic frequency. For a Keplerian disk,  $\kappa = \Omega$ , (3-12) is a corotation resonance.

We note that this paper deals only with dipole field from the star. When higher-order multipole fields are considered, it is conceivable that additional resonances can arise.

### 3.2. Magnetic Torques at Resonances

What are the consequences of the magnetically driven resonances? We have not investigated this issue in detail. The resonances may act as an extra source (in addition to the non-resonant warping torques discussed in §2 and §4) for generating bending waves and spiral waves in the disk. Near the resonances, fluid elements undergo large out-of-plane and radial excursions, which may lead to thickening of the disk<sup>6</sup>.

We can get some insight into the resonances by calculating the magnetic torques at the resonant radii. Consider first the torque associated with the force in eq. (3-2). For a Keplerian disk, the condition  $\Omega_z = \Omega$  is always satisfied. When  $\sin \beta \cos \theta \neq 0$ , there always exists a net (averaged) torque acting on the fluid element, pulling its orbital angular momentum axis toward (or away from) the spin axis (eq. [2-39]). The condition  $\Omega + \Omega_z = \omega$  (or  $2\Omega = \omega$  for a Keplerian disk) specifies a special radius in the disk. To calculate the net torque on the fluid element at this resonant radius, we cannot average  $\phi$  and the spin period independently (as done in §2). Instead we write the torque  $\mathbf{N} = \mathbf{r} \times \mathbf{F}$  as:

$$\begin{aligned} \mathbf{N} = \frac{\zeta \mu B_z}{4\pi r^2} & \left\{ \left[ \sin \theta \cos \omega t (1 - \cos 2\phi) - (\sin \beta \cos \theta + \cos \beta \sin \theta \sin \omega t) \sin 2\phi \right] \hat{x} \right. \\ & \left. + \left[ -\sin \theta \cos \omega t \sin 2\phi + (\sin \beta \cos \theta + \cos \beta \sin \theta \sin \omega t) (1 + \cos 2\phi) \right] \hat{y} \right\}. \quad (3-13) \end{aligned}$$

Following a fluid element we have  $\phi = \Omega t + \phi_0$ . Averaging over time, we find that, at the  $2\Omega = \omega$  resonance, the torque is given by

$$\langle \langle \mathbf{N} \rangle \rangle = \frac{\zeta \mu B_z}{4\pi r^2} \sin \beta \cos \theta \hat{y} - \frac{\zeta \mu B_z}{8\pi r^2} (1 + \cos \beta) \sin \theta (\hat{x} \cos 2\phi_0 + \hat{y} \sin 2\phi_0). \quad (3-14)$$

---

<sup>6</sup>This may be analogous to the Lorentz resonances (which occur when charge particles move around a rotating magnetic field) in the jovian ring (Burns et al. 1985; Schaffer & Burns 1992). However, because of the fluid nature of the disk, the resonances may not lead to sharp edges in the disk.

Thus for each fluid element on the resonant radius, the averaged torque is modified from the “nonresonant” value (the first term in eq. [3-14]). Since different fluid elements in the same ring have different values of  $\phi_0$ , they will experience different torques; if they are allowed to move independent of each other, the ring will eventually disperse. However, if there is strong coupling between the different elements on the ring so that the ring evolve dynamically as an identity, then one should average over  $\phi_0$ , and eq. (3-14) reduces to (2-39). We can similarly consider the torque associated with the magnetic force given in eq. (2-41). At both the  $\Omega = \omega$  and  $2\Omega = \omega$  resonances, in addition to eq. (2-42), there are “resonant” torques which depend on  $\phi_0$  (analogous to eq. [3-14]).

We note that the “nonresonant” torque is nonzero only when  $\sin \beta \neq 0$  (misaligned spin-orbit), while at the  $2\Omega = \omega$  or  $\Omega = \omega$  resonances, the torque can be nonzero even when  $\beta = 0$ . Also note that in general, the “resonant” torque is of the same order of magnitude as the “nonresonant” torque. We shall not consider these resonances in the rest of the paper.

#### 4. DYNAMICS OF WARPING AND PRECESSING DISK

We now study the dynamics of the disk under the influence of the magnetic torques calculated in §2. For concreteness, we shall use the torque expressions of §2.3; using other expressions of §2 would give similar results (although the dependence on angles would be different). We are particularly interested in whether the warping instability can operate in the presence of disk viscosity.

##### 4.1. Criterion for the Warping Instability

Our starting point is the evolution equation for disk tilt  $\hat{l}(r, t)$  (the unit vector perpendicular to the disk annulus at radius  $r$ ) given by Pringle (1992) (see also Papaloizou & Pringle 1983)<sup>7</sup>:

$$\begin{aligned} \frac{\partial \hat{l}}{\partial t} + \left[ V_r - \frac{\nu_1 \Omega'}{\Omega} - \frac{1}{2} \nu_2 \frac{(\Sigma r^3 \Omega)'}{\Sigma r^3 \Omega} \right] \frac{\partial \hat{l}}{\partial r} \\ = \frac{\partial}{\partial r} \left( \frac{1}{2} \nu_2 \frac{\partial \hat{l}}{\partial r} \right) + \frac{1}{2} \nu_2 \left| \frac{\partial \hat{l}}{\partial r} \right|^2 + \frac{\mathbf{N}}{\Sigma r^2 \Omega}. \end{aligned} \quad (4-1)$$

Here  $V_r$  is the radial velocity of the flow,  $\Omega' \equiv d\Omega/dr$ ,  $\nu_1$  is the usual disk viscosity (measuring the  $r$ - $\phi$  stress), and  $\nu_2$  is the viscosity (measuring the  $r$ - $z$  stress) associated with reducing disk tilt. We assume that the timescale for  $\hat{l}$  to change is much longer than the spin period, so that  $\mathbf{N}$  is the

---

<sup>7</sup>Recent study (Ogilvie 1999) indicates that in the nonlinear regime, the warping equation needs to be modified. In effect,  $\nu_1$  and  $\nu_2$  are not the usual vertically averaged viscosities and may depend on the amplitude of the warp.

averaged torque (per unit area) as calculated in §2.3 (The notation  $\langle\langle\cdots\rangle\rangle$  has been suppressed). Using the following relations for a Keplerian disk:

$$V_r = -\frac{3\nu_1}{2r}\mathcal{J}^{-1}, \quad \Sigma = \frac{\dot{M}}{3\pi\nu_1}\mathcal{J}, \quad (4-2)$$

where  $\mathcal{J}$  is a function of  $r$  which approaches unity in the region far from the inner edge of the disk (see Appendix A), and assuming that  $\nu_2/\nu_1$  is independent of  $r$ , we reduce eq. (4-1) to

$$\begin{aligned} \frac{\partial \hat{l}}{\partial t} - \left[ \frac{3\nu_2}{4r} \left( 1 + \frac{2r\mathcal{J}'}{3\mathcal{J}} \right) + \frac{3\nu_1}{2r} (\mathcal{J}^{-1} - 1) \right] \frac{\partial \hat{l}}{\partial r} \\ = \frac{1}{2}\nu_2 \frac{\partial^2 \hat{l}}{\partial r^2} + \frac{1}{2}\nu_2 \left| \frac{\partial \hat{l}}{\partial r} \right|^2 + \frac{\mathbf{N}}{\Sigma r^2 \Omega}. \end{aligned} \quad (4-3)$$

We rewrite the magnetic torques in eqs. (2-33), (2-34) as

$$\frac{\mathbf{N}_{\text{prec}}}{\Sigma r^2 \Omega} = -\Omega_p \cos \beta \hat{\omega} \times \hat{l}, \quad \Omega_p = \frac{\mu^2}{\pi^2 r^7 \Omega \Sigma D} \sin^2 \theta, \quad (4-4)$$

$$\frac{\mathbf{N}_{\text{warp}}}{\Sigma r^2 \Omega} = -\Gamma_w \cos \beta \sin \beta \hat{y}, \quad \Gamma_w = \frac{\zeta \mu^2}{4\pi r^7 \Omega \Sigma} \cos^2 \theta. \quad (4-5)$$

At this stage  $\hat{l}$  is no longer useful as a coordinate axis, so we consider a different cartesian coordinate system where  $\hat{\omega}$  is the  $z'$ -axis (see Fig. 1). In this coordinate system, we write

$$\hat{l} = (\sin \beta \cos \gamma, \sin \beta \sin \gamma, \cos \beta), \quad (4-6)$$

which defines the local twist angle  $\gamma$ . For small tilt angle ( $\beta \ll 1$ ), eq. (4-3) simplifies to

$$\frac{\partial W}{\partial t} - \frac{3\nu_2}{4r} \frac{\partial W}{\partial r} = \frac{1}{2}\nu_2 \frac{\partial^2 W}{\partial r^2} - i\Omega_p W + \Gamma_w W, \quad (4-7)$$

where  $W \equiv \beta e^{i\gamma}$ , and we have set  $\mathcal{J} = 1$  (far from the inner edge of the disk) – using a more rigorous  $\mathcal{J}$  would only affect the numerical coefficient in front of the  $\partial W/\partial r$  term.

To derive the instability criterion, we consider the WKB solution of the form (valid for  $kr \gg 1$ )

$$W \propto \exp(i\sigma t + ikr). \quad (4-8)$$

Substituting into (4-7), we obtain the dispersion relation

$$\sigma = \left( \frac{3\nu_2}{4r} k - \Omega_p \right) + i \left( \frac{1}{2}\nu_2 k^2 - \Gamma_w \right). \quad (4-9)$$

For the instability to grow, we require  $\text{Im}(\sigma) < 0$ , or

$$\Gamma_w > \frac{1}{2}\nu_2 k^2 \iff \text{Instability}. \quad (4-10)$$



Since the radial wavelength is restricted to  $\lambda \leq r$ , or  $k \geq 2\pi/r$ , the instability criterion becomes

$$\Gamma_w > 2\pi^2 \frac{\nu_2}{r^2} \iff \text{Instability.} \quad (4-11)$$

This criterion has a simple physical interpretation: The magnetic torque drives the growth of disk tilt on a timescale  $\Gamma_w^{-1}$ , while viscosity tries to reduce the tilt on a timescale  $r^2/\nu_2$  (which is of the same order as the radial drift time of the flow,  $r/|V_r|$ , if  $\nu_2$  is of the same order as  $\nu_1$ ). Instability requires  $\Gamma_w^{-1} \lesssim r^2/\nu_2$ .

Using (4-2) and (4-5), and assuming that  $\nu_2/\nu_1$  is independent of  $r$ , we can further reduce (4-11) to

$$r < r_w = \left( \frac{3\zeta \cos^2 \theta \nu_1}{8\pi^2 \mathcal{J} \nu_2} \right)^{2/7} \left( \frac{\mu^4}{GM\dot{M}^2} \right)^{1/7}. \quad (4-12)$$

This indicates that inside the critical *warping radius*  $r_w$ , the magnetic torque can overcome the viscous force and make the disk tilt grow. Moreover, with the expected<sup>8</sup>  $\zeta \sim 1$ ,  $\nu_1/\nu_2 \sim 1$  and  $\mathcal{J} \leq 1$ , the warping radius is of the same order of magnitude as the magnetosphere radius  $r_m$  (see eq. [1-1] and Appendix B for a discussion of the magnetosphere radius for arbitrary geometry). Thus, as the disk approaches the magnetosphere, it will tend to be tilted with respect to the stellar spin even if at large radii the disk normal is aligned with the spin axis.

Similar analysis can be applied to the case where the disk is nearly antiparallel to the spin ( $\pi - \beta \ll 1$ ). If we define  $W \equiv (\pi - \beta)e^{i\gamma}$ , then eq. (4-7) remains valid except the sign in front of  $i\Omega_p W$  changes. We obtain the same instability criterion as above. Thus, an antiparallel disk tends to be driven toward a perpendicular configuration near the magnetosphere radius.

## 4.2. Magnetic Bardeen-Petterson Effect

A tilted disk will be driven into precession by the torque  $\mathbf{N}_{\text{prec}}$  with  $\boldsymbol{\Omega}_{\text{prec}} = -\Omega_p \cos \beta \hat{\omega}$  (see eq. [4-4]). What is the effect of this precession on the disk tilt? An analogy can be made with the behavior of a disk undergoing Lense-Thirring precession around a rotating black hole (or any compact object) (Bardeen & Petterson 1975; Kumar & Pringle 1985; Pringle 1992; Scheuer & Feiler 1996).

The gravitomagnetic force from the rotating object (with spin angular momentum  $\mathbf{J} = J\hat{\omega}$ ) drives the precession of the misaligned disk at angular frequency  $\boldsymbol{\Omega}_{\text{LT}} = 2G\mathbf{J}/(c^2 r^3)$ . Bardeen & Petterson (1975) pointed out that the action of viscosity on the differentially precessing disk tends to align the rotation of the inner disk with the spin axis of the central object. The

---

<sup>8</sup>For Keplerian and inviscid (or very nearly so) disks, resonance between the epicyclic frequency and orbital frequency leads to  $\nu_2/\nu_1 \simeq 1/(2\alpha^2) \gg 1$ . However, the resonance is delicate and might be destroyed by the effects of general relativity, self-gravity, magnetic fields and turbulence. See Ogilvie (1999) for a discussion.

Bardeen-Petterson radius  $r_{\text{BP}}$ , that is, loosely speaking, the radius inside which the disk aligns with the spin, is obtained by equating the precessional time  $\Omega_{\text{LT}}^{-1}$  and the viscous time  $r^2/\nu_2$  (Scheuer & Feiler 1996), i.e.,

$$r_{\text{BP}} = \frac{2GJ}{c^2\nu_2}. \quad (4-13)$$

However, the transition from the warped outer disk to the aligned inner disk is rather broad, and for this reason the timescale to achieve the Bardeen-Petterson alignment is much larger than the precession timescale at  $r_{\text{BP}}$  (Kumar & Pringle 1985; Pringle 1992). Numerical simulations (Pringle 1992) indicate that a steady state is achieved on a time scale of order  $(10 - 100)\Omega_{\text{LT}}^{-1}$  (evaluated at  $r_{\text{BP}}$ ).

Now consider the effect of magnetically driven precession<sup>9</sup>. Setting  $\Omega_p$  equal to  $\nu_2/r^2$ , we obtain the magnetic Bardeen-Petterson radius:

$$r_{\text{MBP}} = \left( \frac{3 \sin^2 \theta \nu_1}{\pi \mathcal{J} D \nu_2} \right)^{2/7} \left( \frac{\mu^4}{GMM^2} \right)^{1/7}. \quad (4-14)$$

Inside  $r_{\text{MBP}}$ , the combined effect of viscosity and precession tends to align the disk normal with the spin axis. We see that typically  $r_{\text{MBP}}$  is of the same order as  $r_w$  (the warping radius) and  $r_m$  (the magnetosphere radius). Thus the precessional torque has an opposite effect on the disk tilt as the warping torque discussed in §5.1. However, because of the broad warp-alignment transition expected for the magnetic Bardeen-Petterson effect and the long timescale involved, we expect that the precession-induced alignment will be overwhelmed by the warping instability.

## 5. EFFECT ON THE SPIN EVOLUTION

How does the magnetically warped and precessing disk affect the spin evolution of the central star? The angular momentum of the accreting gas is deposited at the magnetospheric boundary and transferred to the central object. In addition, there are back-reactions on the star associated with the magnetic torques on the disk. Thus the spin angular velocity  $\boldsymbol{\omega}$  evolves according to

$$\frac{d}{dt}(I\boldsymbol{\omega}) = \dot{M}(GMr_m)^{1/2}\hat{l} - \mathcal{N}_{\text{prec}} - \mathcal{N}_{\text{warp}}, \quad (5-1)$$

where  $I$  is the moment of inertia,  $\mathcal{N}_{\text{prec}}$  and  $\mathcal{N}_{\text{warp}}$  are the total warping and precessional torques acting on the disk<sup>10</sup>. To calculate  $\mathcal{N}_{\text{prec}}$  and  $\mathcal{N}_{\text{warp}}$ , we need to know the tilt angle  $\beta$  as a

---

<sup>9</sup>In some systems (such as accreting neutron stars with weak magnetic fields), the Lense-Thirring precession dominates (See §6). But here we neglect  $\Omega_{\text{LT}}$ .

<sup>10</sup>In (5-1) we have neglected possible magnetic torque [as in the Ghosh & Lamb (1979a,b) picture] associated closed magnetic field lines that thread the disk and connect the star. Such magnetic torque can be included by modifying the first term on the right-hand-side of (5-1) to  $\dot{M}\sqrt{GMr_m}f\hat{l}$ , where  $f$  is a dimensionless function which depends on the ratio  $\omega/\Omega(r_m)$  [See, e.g., eq. (35) of Lai (1998) and references therein].

function of  $r$ . In principle this can be obtained by solving the tilt equation (4-1) or (4-3). But note that since the torques per unit area (eqs. [2-33]-[2-34]) are steep functions of  $r$ , we can assume, as a first approximation, that  $\beta$  is independent of  $r$  near  $r_m$ . We then find

$$\mathcal{N}_{\text{prec}} = \int_{r_m}^{\infty} 2\pi r \mathbf{N}_{\text{prec}} dr = -\frac{4\mu^2}{3\pi r_m^3} \sin^2\theta \cos\beta (\hat{\omega} \times \hat{l}), \quad (5-2)$$

and

$$\mathcal{N}_{\text{warp}} = \int_{r_m}^{\infty} 2\pi r \mathbf{N}_{\text{warp}} dr = -\frac{\zeta\mu^2}{12r_m^3} \cos^2\theta \sin 2\beta \hat{y} = -\frac{\zeta\mu^2}{6r_m^3} \cos^2\theta \cos\beta [\hat{\omega} - (\hat{\omega} \cdot \hat{l})\hat{l}]. \quad (5-3)$$

Note that the ratio of the characteristic magnetic torque,  $\mathcal{N}_{\text{mag}} = \mu^2/r_m^3$ , and the characteristic accretion torque,  $\mathcal{N}_{\text{acc}} = \dot{M}\sqrt{GM r_m}$ , is

$$\frac{\mathcal{N}_{\text{mag}}}{\mathcal{N}_{\text{acc}}} = \left( \frac{\mu^2}{\dot{M}\sqrt{GM}} \right) \frac{1}{r_m^{7/2}} = \eta^{-7/2}, \quad (5-4)$$

[see eq. (1-1) and Appendix B]. The spin evolution equation can then be written as

$$\begin{aligned} \frac{d}{dt}(I\boldsymbol{\omega}) &= \mathcal{N}_{\text{acc}} \left[ 1 + \frac{\zeta \cos^2\theta}{6\eta^{7/2}} \sin^2\beta \right] \cos\beta \hat{\omega} \\ &+ \mathcal{N}_{\text{acc}} \left[ \frac{\zeta \cos^2\theta}{6\eta^{7/2}} \cos^2\beta - 1 \right] \sin\beta \hat{\omega}_{\perp} \\ &- \mathcal{N}_{\text{acc}} \left( \frac{4}{3\pi\eta^{7/2}} \sin^2\theta \cos\beta \right) \hat{l} \times \hat{\omega}, \end{aligned} \quad (5-5)$$

where  $\hat{\omega}_{\perp}$  is a unit vector perpendicular to  $\hat{\omega}$  and lies in the plane spanned by  $\hat{l}$  and  $\hat{\omega}$  (see Fig. 1). The physical effects of the three terms on the right-hand-side of (5-5) are evident: The first term is responsible to the spin-up or spin-down (depending on the sign of  $\cos\beta$ ) of the star; the second term tends to align or misalign the spin axis with the disk axis<sup>11</sup>, and the third term induces precession of the star's spin axis  $\hat{\omega}$  around  $\hat{l}$ . The timescales associated with these changes of  $\boldsymbol{\omega}$  (spin-up/spin-down, alignment/misalignment and precession) are all of order

$$\tau_{\text{spin}} = \frac{I\omega}{\mathcal{N}_{\text{acc}}} = \frac{I\omega}{\dot{M}\sqrt{GM r_m}}. \quad (5-6)$$

This spin-changing timescale is typically much longer than the timescale associated with changing the disk orientation (see §4 and §6).

Note that eq. (5-6) represents the instantaneous spin-up/spin-down timescale (i.e., at a given  $\beta$ ). If the disk inclination  $\beta$  wanders around  $90^\circ$ , we expect the secular spin-up of the star to be slower (see §6).

---

<sup>11</sup>Since the timescale to change  $\hat{\omega}$  is much longer than the timescale to change  $\hat{l}$ , the change of the tilt angle  $\beta$  is determined by the dynamics of  $\hat{l}$  rather than  $\hat{\omega}$  (see eq. [2-36] and §4).

## 6. ASTROPHYSICAL APPLICATIONS

In this section we discuss/speculate several possible applications of our theory. While preliminary, they demonstrate the potential importance of the physical effects uncovered in previous sections.

### 6.1. Spin Evolution of Disk-Fed X-Ray Pulsars

Recent long-term, continuous monitoring of accreting X-ray pulsars with the BATSE instrument on the Compton Gamma Ray Observatory has revealed a number of puzzling behaviors of the spins of these accreting, magnetized neutron stars (see Bildsten et al. 1997 and references therein). Several well-measured disk-fed systems (e.g., Cen X-3, GX 1+4 and 4U 1626-67) display sudden transitions between episodes of steady spin-up and spin-down, with the absolute values of spin torques approximately equal (to within a factor of two). Of special interest is the observed anticorrelation between the torque and X-ray luminosity during the spin-down phase of GX 1+4 (i.e., the torque becomes more negative as the luminosity increases; Chakrabarty et al. 1997). These features are at odds with previous theoretical models, according to which the neutron star must be near spin-equilibrium in order to experience both spin-up and spin-down (e.g., Ghosh & Lamb 1979a,b; see also Yi, Wheeler & Vishniac 1997; Torkelsson 1998; Lovelace et al. 1998). It has been noted that the observational data can be nicely explained if the disk can somehow change its sense of rotation (Nelson et al. 1997) — This poses a significant theoretical problem, since the disk formed in a Roche lobe overflow has a well-defined direction of rotation. It has been suggested (Van Kerkwijk et al. 1998) that the disk reversal may be caused by the radiation-driven warping instability (Pringle 1996), although the extent and timescale of the reversal remain unclear. (Recall that one expects the radiation-driven instability to operate only at large radii; Pringle 1996.) Also, since the radiation driven warping does not directly depends on the spin orientation, it is not clear why the disk prefers to wander around the perpendicular state ( $\beta = 90^\circ$ ).

Here we suggest that the magnetically driven warping instability uncovered in this paper plays an important role in the determining the spin behaviors of accreting X-ray pulsars. The magnetosphere is located at

$$r_m = \eta \left( \frac{\mu^4}{GM\dot{M}^2} \right)^{1/7} = \left( 3.4 \times 10^8 \text{ cm} \right) \eta \mu_{30}^{4/7} M_{1.4}^{-1/7} \dot{M}_{17}^{-2/7}, \quad (6-1)$$

and we shall consider  $\eta$  to be a constant of order unity (see Appendix B). Here  $\mu_{30}$ ,  $M_{1.4}$  and  $\dot{M}_{17}$  are the neutron star’s magnetic moment, mass and accretion rate in units of  $10^{30} \text{ G cm}^3$ ,  $1.4M_\odot$  and  $10^{17} \text{ g s}^{-1}$ , respectively. Near the magnetosphere, the disk lies in the so-called “middle” (gas pressure and scattering dominated) region of the  $\alpha$ -disk solution (Shakura & Sunyaev 1973; Novikov & Thorne 1973). The surface density of the disk is

$$\Sigma = \left( 1.7 \times 10^3 \text{ g cm}^{-2} \right) \alpha^{-4/5} M_{1.4}^{1/5} \dot{M}_{17}^{3/5} r_8^{-3/5} \mathcal{J}^{3/5}, \quad (6-2)$$

where  $r_8 = r/(10^8 \text{ cm})$ , and the possible effect of a threaded magnetic field can be included in the definition of  $\mathcal{J}$  (see Appendix A). The growth rate of the magnetic warping instability (eq. [4-5]) is given by

$$\begin{aligned}\Gamma_w &= (0.035 \text{ s}^{-1}) (\zeta \cos^2 \theta) \alpha^{4/5} \mu_{30}^2 M_{1.4}^{-7/10} \dot{M}_{17}^{-3/5} r_8^{-49/10} \mathcal{J}^{-3/5} \\ &= \left( \frac{1}{5.3 \text{ day}} \right) (\zeta \cos^2 \theta) \left( \frac{\alpha}{0.01} \right)^{4/5} \mu_{30}^{-4/5} \dot{M}_{17}^{4/5} \left( \frac{r_m}{\eta r} \right)^{49/10} \mathcal{J}^{-3/5}.\end{aligned}\quad (6-3)$$

As discussed in §2 and §4, the magnetic torque tends to drive the inner region (near the magnetosphere) of the disk toward a perpendicular configuration ( $\beta = 90^\circ$ ) on a timescale of order  $\Gamma_w^{-1}$ . Indeed, the  $\beta = \pi/2$  state represents an “attractor”. In the idealized situation (each disk ring evolves independent of each other), the tilt of a nearly orthogonal disk evolves according to

$$\frac{d\Delta\beta}{dt} = \Gamma_w \sin \beta \cos \beta \simeq -\Gamma_w \Delta\beta, \quad (6-4)$$

where  $\Delta\beta \equiv \beta - \pi/2$  (see eq. [2-36]). The star can then spin-up or spin-down, depending on the whether  $\beta < 90^\circ$  or  $\beta > 90^\circ$  [see eq. (5-5)]:

$$I\dot{\omega} = \mathcal{N}_{\text{acc}} \left[ 1 + \frac{\zeta \cos^2 \theta}{6\eta^{7/2}} \sin^2 \beta \right] \cos \beta. \quad (6-5)$$

The characteristic spin-up/spin-down time scale (eq. [5-6]) is

$$\tau_{\text{spin}} = (7.9 \times 10^3 \text{ yrs}) \eta^{-1/2} M_{1.4}^{-3/7} I_{45} \mu_{30}^{-2/7} \dot{M}_{17}^{-6/7} \left( \frac{1 \text{ s}}{P_s} \right), \quad (6-6)$$

where  $P_s$  is the spin period, and  $I_{45} = I/(10^{45} \text{ g cm}^2)$ .

In our picture, the observed sign switching of  $\dot{\omega}$  in several X-ray pulsars is associated with the “wandering” of  $\beta$  around the “preferred” value ( $\beta = 90^\circ$ ). Such “wandering” needs not be periodic: Consider a disk initially at  $\beta = 90^\circ$ . Imagine that a perturbation in the accretion induces a negative (not necessarily small)  $\Delta\beta = \beta - 90^\circ$  — This is achieved on a viscous timescale (which is of the same order of magnitude as  $\Gamma_w^{-1}$  at the inner disk edge; see §4.1). The star spins up. The magnetic torque then drives  $\beta$  toward  $90^\circ$  on the timescale of  $\Gamma_w^{-1}$ , at which point another perturbation (which cannot be faster than  $\Gamma_w^{-1}$ ) can induce another  $\Delta\beta$ , which can be either negative or positive, and the star will then continue to spin-up or switch to spin-down. We expect that the timescale of the switching between spin-up and spin-down is of order a few times  $\Gamma_w^{-1}$  (evaluated at the inner disk boundary). For  $\alpha \sim 0.1 - 0.01$  and  $\dot{M}_{17} \sim 0.1$ ,  $\mu_{30} \sim 1$  (typical of X-ray pulsars), eq. (6-3) gives  $\Gamma_w^{-1} \sim 5 - 30$  days (for  $\zeta \cos^2 \theta = 1$ ), comparable to what is observed in Cen X-3 ( $P_s = 4.8 \text{ s}$ ) (Bildsten et al. 1997). For 4U 1626-67 ( $P_s = 7.6$ ) and GX 1+4 ( $P_s = 120 \text{ s}$ ), the sign of  $\dot{\omega}$  switches once in 10 – 20 yr. Since equation (6-3) is uncertain and depends on many parameters, it is conceivable that such long switching time can be accommodated (e.g., with  $\zeta \cos^2 \theta = 0.1$ ,  $\alpha = 0.01$ ,  $\dot{M}_{17} = 0.1$  and  $\mu_{30} = 10$ , we find  $\Gamma_w^{-1} \simeq 6$  years).

Note that eq. (6-6) represents the “instantaneous” spin-up/spin-down time of the neutron star. Since the outer disk has a well-defined direction (presumably with  $\beta < 90^\circ$ ), the inner disk will unlikely spend equal amount of time in the prograde ( $\beta < 90^\circ$ ) phase and the retrograde ( $\beta > 90^\circ$ ) phase. Thus we expect that on a longer time scale (longer than the disk reversal time  $\Gamma_w^{-1}$ ), the neutron star will experience secular spin-up. This expectation is borne out by observations, although it is difficult to predict the long-term spin-up rate.

A full study or simulation of the nonlinear behavior of the inner disk tilt would be desirable to make more meaningful comparison with observations. But our discussion and estimate given above indicates that magnetically driven warping may be a crucial ingredient in explaining the spin behaviors of disk-fed X-ray pulsars. Other physical effects (such as radiation driven warping and propeller effect; Van Kerkwijk et al. 1998, Lovelace et al. 1998) may also play a role.

## 6.2. Weakly Magnetized Neutron Stars: Quasi-Periodic Oscillations

Rapid variability in low-mass X-ray binaries (LMXBs), containing weakly magnetized ( $B \sim 10^7 - 10^9$  G) neutron stars, has been studied since the discovery of the so-called horizontal-branch oscillations (HBOs) in a subclass of LMXBs called Z sources (van der Klis et al. 1985; Hasinger & van der Klis 1989). The HBOs are quasi-periodic oscillations (QPOs) (with the  $Q$ -value  $\nu/\Delta\nu$  of order a few, and rms amplitude  $\lesssim 10\%$ ) which manifest as broad Lorentzian peaks in the X-ray power spectra with centroid frequencies in the range of 15 – 60 Hz which are positively correlated with the inferred mass accretion rate (see van der Klis 1995 for a review). For many years, the standard interpretation for the HBOs has been based on the magnetosphere beat-frequency model, first advocated by Alpar & Shaham (1985) and Lamb et al. (1985), in which the HBO is identified with the difference frequency between the Keplerian frequency at the magnetospheric boundary and the spin frequency of the neutron star (see Ghosh & Lamb 1992 for a review). However, recent observations of kHz QPOs (500 – 1200 Hz) in at least eighteen LMXBs by the Rossi X-ray Timing Explorer (RXTE) have called into question this interpretation of HBOs (see van der Klis 1998a,b for review). The kHz QPOs (with  $Q$  up to 100 and rms amplitude up to 20%) often come in pairs, and both frequencies move up and down as a function of photon count rate, with the separation frequency roughly constant (The clear exceptions are Sco X-1 and 4U 1608-52; van der Klis et al. 1997, Mendez et al. 1998a). In most Z sources, the 15-60 Hz HBOs appear simultaneously with the kHz QPOs, while in several atoll sources (which are thought to have weaker magnetic fields and smaller accretion rates than the Z sources), broad peaks at 10 – 50 Hz in the power spectra (similar to the HBOs in the Z sources) have also been detected at the same time when the kHz QPOs appear. While the origin of the kHz QPOs is uncertain, it is natural to associate the higher frequency QPO with the orbital motion at the inner edge (perhaps the magnetosphere boundary) of the accretion disk, and the lower-frequency QPO may result from the (perhaps imperfect) beat between the Kepler frequency and the neutron

star spin frequency<sup>12</sup> — This beat frequency interpretation is supported by the observations of a third, nearly coherent QPO which occurs during X-ray bursts, at a frequency approximately equal to the frequency difference between the twin kHz peaks or twice that value. (An exception is 4U 1636-53, Mendez et al. 1998b.) Clearly, if this generic identification of kHz QPOs is correct, the beat between the  $\sim 1$  kHz Keplerian frequency at the disk inner edge and the  $\sim 300$  Hz spin frequency cannot produce the 10 – 60 Hz low-frequency QPOs (LFQPOs: HBOs in the Z sources and similar features in the atoll sources), unless one postulates (Miller, Lamb & Psaltis 1998) that the inner disk edge lies inside the magnetosphere and is unaffected by the magnetic field.

Stella and Vietri (1998) suggested that the 10 – 60 Hz LFQPOs are associated with Lense-Thirring precession of the inner accretion disk around the rotating neutron star. Assuming that the low-frequency QPO and the kHz QPOs are generated at the same radius in the disk, one obtains, to leading order,  $\Omega_{\text{LT}} = (2I\omega/Mc^2)\Omega^2$  (where  $\Omega$ ,  $\Omega_{\text{LT}}$  and  $\omega$  are the orbital, Lense-Thirring, and spin angular frequencies, respectively). Thus the LFQPO frequency depends quadratically on the kHz QPO frequency. (The classical precession associated with spin-induced oblateness of the star, as well as relativistic effect beyond the Lense-Thirring formula, both can introduce small correction to this correlation; see Stella & Vietri 1998, Morsink & Stella 1999.) This is consistent with observations of several sources (e.g., the Z sources GX17+2, GX5-1, Sco X-1, and the atoll source 4U1728-34; see Ford & van der Klis 1998, Psaltis et al. 1999 and references therein)<sup>13</sup>.

For the Lense-Thirring interpretation of HBOs to be viable, the inner disk must be tilted with respect to the stellar spin axis. The Bardeen-Petterson effect tends to keep the inner region of the disk [inside  $r_{\text{BP}}$ , typically at  $(100 - 1000)GM/c^2$ ] co-planar with the star (Bardeen & Petterson 1975). Radiation driven warping (Pringle 1996) is only effective at large disk radii. While global disk warping modes may exist with nonzero tilt near the inner disk boundary (Ipser 1996; Marković & Lamb 1998), an external driving force is needed to excite them.

Here we suggest that the magnetic warping torque provides a natural driver for the disk tilt near the inner accretion disk<sup>14</sup>. For typical parameters of LMXBs, the magnetosphere is located

---

<sup>12</sup>See Stella & Vietri (1999) for an alternative interpretation of the lower QPO peak which does not involve beating.

<sup>13</sup>Observations indicate that the ratio  $I/M$  required to fit the expected  $\Omega_{\text{LT}} - \Omega$  relation is a factor of 2 – 4 larger than allowed by neutron star equation of state. This situation can be improved if the observed LFQPO frequency is the second harmonic of the fundamental precession frequency (See, e.g., Stella & Vietri 1998, Morsink & Stella 1999, Psaltis et al. 1999). In some Z sources, one requires that the observed HBO frequency is four times the fundamental precession frequency in order to produce reasonable  $I/M$ . Alternatively, the spin frequency is twice of what is inferred from the difference between the twin kHz QPOs — This would make the beat frequency interpretation of the lower kHz peak invalid. It would be interesting to search for “sub-harmonic” feature of the HBOs in the power spectra (see Ford & van der Klis 1998 for possible evidence of such a sub-harmonic feature in 4U 1728-34).

<sup>14</sup>Vietri and Stella (1998) suggested that if the accretion disk is inhomogeneous, diamagnetic blobs can be lifted above the equatorial plane through resonant interaction with the star’s magnetic field near the the corotation radius. See Appendix C.

at<sup>15</sup>

$$r_m = (18 \text{ km}) \eta \mu_{26}^{4/7} M_{1.4}^{-1/7} \dot{M}_{17}^{-2/7} \quad (6-7)$$

where  $\mu_{26} = \mu/(10^{26} \text{ G cm}^3)$ . Assuming that near the magnetosphere the disk is described by the “inner region” (radiation and scattering dominated) solution of  $\alpha$ -disk (Shakura & Sunyaev 1973; Novikov & Thorne 1973), we have for the disk surface density and half-thickness

$$\Sigma = (105 \text{ g cm}^{-2}) \alpha^{-1} M_{1.4}^{-1/2} \dot{M}_{17}^{-1} r_6^{3/2} \mathcal{J}^{-1}, \quad (6-8)$$

$$H = (1.1 \text{ km}) \dot{M}_{17} \mathcal{J}, \quad (6-9)$$

where  $r_6 = r/(10^6 \text{ cm})$ . The growth rate of the magnetic warping instability (eq. [4-5]) is then

$$\begin{aligned} \Gamma_w &= (555 \text{ s}^{-1}) (\zeta \cos^2 \theta) \alpha \mu_{26}^2 \dot{M}_{17} r_6^{-7} \mathcal{J} \\ &= (1.0 \text{ s}^{-1}) (\zeta \cos^2 \theta) \left(\frac{\alpha}{0.1}\right) M_{1.4} \mu_{26}^{-2} \dot{M}_{17}^3 \left(\frac{r_m}{\eta r}\right)^7 \mathcal{J}. \end{aligned} \quad (6-10)$$

The magnetic effect also results in a precessional torque on the disk. From eq. (2-35) and using (6-8)-(6-9), we find that the precession frequency associated with this magnetic torque is

$$\begin{aligned} \nu_{\text{prec}} &= -(0.21 \text{ Hz}) (\sin^2 \theta \cos \beta) \left(\frac{\alpha}{0.1}\right) M_{1.4} \mu_{26}^{-2} \dot{M}_{17}^3 \left(\frac{r_m}{\eta r}\right)^7 D^{-1} \mathcal{J} \\ &= -(0.60 \text{ Hz}) (\sin^2 \theta \cos \beta) \left(\frac{\alpha}{0.1}\right) M_{1.4}^{3/7} \mu_{26}^{-12/7} \dot{M}_{17}^{20/7} \eta^{1/2} \left(\frac{r_m}{\eta r}\right)^7 \mathcal{J}^{1/2}, \end{aligned} \quad (6-11)$$

where in the second equality we have used  $D = (2H/r_m)^{1/2}$  [see eq. (2-4)]. This should be compared with the Lense-Thirring precession frequency

$$\begin{aligned} \nu_{\text{LT}} &= (44.4 \text{ Hz}) I_{45} r_6^{-3} \left(\frac{\nu_s}{300 \text{ Hz}}\right) \\ &= (8.1 \text{ Hz}) M_{1.4}^{3/7} I_{45} \mu_{26}^{-12/7} \dot{M}_{17}^{6/7} \left(\frac{\nu_s}{300 \text{ Hz}}\right) \left(\frac{r_m}{\eta r}\right)^3, \end{aligned} \quad (6-12)$$

where  $\nu_s$  is the spin frequency. Note that for  $\beta < 90^\circ$  the magnetically driven precession is opposite to the stellar spin axis (thus the negative sign in eq. [6-11]), while Lense-Thirring precession is in the same direction as the spin. For a given source, the magnitude of  $|\nu_{\text{prec}}|$  is typically smaller than  $\nu_{\text{LT}}$ , but it becomes increasingly important with increasing  $\dot{M}$  (since  $\nu_{\text{LT}} \propto \dot{M}^{6/7}$  while  $\nu_{\text{prec}} \propto \dot{M}^{20/7}$ ). This may explain the observed flattening of the correlation between the LFQPO frequency and kHz QPO frequency as the latter increases<sup>16</sup>.

---

<sup>15</sup>Note that since  $r_m$  is so close to the inner-most stable orbit, general relativistic effect tends to move the inner disk edge to a radius larger than what is given in (6-7); see Lai (1998). Here we shall neglect such complication.

<sup>16</sup>Since the classical precession rate due to the oblateness of the star is negative (for  $\cos \beta > 0$ ) and scales as  $r^{-7/2}$  (while  $\nu_{\text{LT}} \propto r^{-3}$ ) (Stella & Vietri 1998, Morsink & Stella 1999), it may also explain this observed flattening, provided that the spin frequency is much higher than inferred from the kHz QPOs and the burst QPOs. However, because of the similar power-law indices ( $r^{-7/2}$  vs.  $r^{-3}$ ), it is difficult to explain why the  $\nu_{\text{LFQPO}} \propto \nu_{\text{kHzQPO}}^2$  scaling breaks down only at very high kHz QPO frequency (Psaltis et al. 1999).



We note that although our qualitative conclusion that magnetic effect can induce tilt of the inner accretion disk and therefore facilitate its precession is robust, the analytical expressions given in this subsection only serve as an order-of-magnitude estimate which indicates the potential importance of the magnetically driven precession. More detailed calculations (including global mode analysis) are needed to make more meaningful comparison with observational data. In addition to the intrinsic uncertainties associated with the  $\alpha$ -disk model and the magnetosphere boundary layer, there are two complications that may prove important for LMXBs: (i) General relativistic effect can modify the inner radius of the disk so that it is not just determined by magnetic-plasma stress balance (Lai 1998); (ii) The magnetic field is not expected to be dipolar. This comes about either because of the multipole fields from the central star, or, even if the intrinsic stellar field is dipolar, the (partially diamagnetic) disk can enhance the field in the boundary layer (Lai, Lovelace & Wasserman 1999).

### 6.3. Super-Orbital Periods in X-ray Binaries

Here and in §6.4 we speculate upon two additional applications of our theory.

Many X-ray binaries are known to exhibit long-term cycles in their X-ray or optical luminosities (see Priedhorsky & Holt 1987 and references therein). Of particular interest is the well-established “third” period (longer than the orbital period) in Her X-1 (35 d) (Tananbaum et al. 1972), LMC X-4 (30.5 d) (Lang et al. 1981) and SS433 (164 d) (Margon 1984). It is generally thought that these super-orbital periods result from the precession of a tilted accretion disk. For Her X-1, Katz (1973) proposed that the precession was forced by the torque from the companion star, but left unexplained the origin of the disk’s misalignment with respect to the orbital plane. Recently it has been suggested that the radiation-driven warping instability (Pringle 1996) is responsible for producing warped, precessing disks in many X-ray binaries which exhibit long-term cycles (Maloney & Begelman 1997; Wijers & Pringle 1998).

It is likely that magnetic torque plays a role in driving the warping of the inner disk. The observed systematic variation of the X-ray pulse profile of Her X-1 requires the inner edge of the disk to be significantly warped (Sheffer et al. 1992; Deeter et al. 1998 and references therein). In addition, the magnetically driven precession frequency is

$$\nu_{\text{prec}} = - \left( \frac{1}{26 \text{ day}} \right) (\cos \beta \sin^2 \theta) \left( \frac{\alpha}{0.01} \right)^{4/5} \mu_{30}^{-4/5} \dot{M}_{17}^{4/5} \left( \frac{r_m}{\eta r} \right)^{49/10} \mathcal{J}^{-3/5} D^{-1}, \quad (6-13)$$

where  $r_m$  is the magnetosphere radius [eq. (6-1)], and we have adopted the “middle region” solution of the  $\alpha$ -disk (near the inner edge of the disk,  $D \sim 0.2$ ). This is comparable to the observed super-orbital periods. Moreover, the magnetically driven precession is retrograde with respect to the direction of rotation of the disk, in agreement with observations. Of course, the precession rate is a function of  $r$  and  $\beta$ , so a modal analysis is needed to determine the global precession period.

### 6.4. T Tauri Stars

It is well established that classical T Tauri stars (CTTS) have circumstellar disks; Evidence also exists for magnetospheric accretion induced by the stellar magnetic field (e.g., Hartmann 1998). For typical parameters ( $M \simeq 0.5 M_\odot$ ,  $R \simeq 2R_\odot$ ,  $\dot{M} = 10^{-9} - 10^{-7} M_\odot \text{ yr}^{-1}$ , and surface field  $B_\star \sim 1 \text{ kG}$ ), the magnetosphere is located at a few stellar radii. Using  $\mu = B_\star R^3$ , we find that the growth time for the warping instability at the inner region of the disk is given by [see eq. (4-5)]

$$\Gamma_w^{-1} = (6.5 \text{ days}) \left( \frac{1 \text{ kG}}{B_\star} \right)^2 \left( \frac{2R_\odot}{R} \right)^6 \left( \frac{M}{0.5M_\odot} \right)^{1/2} \left( \frac{r}{8R_\odot} \right)^{11/2} \left( \frac{\Sigma}{1 \text{ g cm}^{-2}} \right) (\zeta \cos^2 \theta)^{-1}. \quad (6-14)$$

The precession period of the tilted disk (see eq. [2-35]) is of the same order of magnitude as  $\Gamma_w^{-1}$ . The surface density  $\Sigma$  is unknown, but reasonable estimates give  $\Sigma \sim 1 - 100 \text{ g cm}^{-2}$  (Hartmann 1998). Therefore  $\Gamma_w^{-1}$  ranges from days to years, much shorter than the lifetime of T Tauris stars ( $\sim 10^6$  years).

It has been observed that the photometric periods (5 – 10 days) of CTTS vary (by as much as 30%) on a timescale of weeks (Bouvier et al. 1995). The origin of this variability is unknown. If we interpret the photometric period as the orbital period at the magnetosphere boundary (Bouvier et al. 1995), then we may understand the period variation in the context of warped, precessing disks: As the inner disk warps and precesses, it experiences different stellar magnetic field, and thus the inner disk radius varies.

It is also of interest to consider the effect of magnetically driven warping on the rotation of T Tauri stars. The projected rotation velocity of CTTS with masses  $M \lesssim 1 M_\odot$  is about  $20 \text{ km s}^{-1}$ , only 10% of the breakup speed (e.g., Bertout 1989). This is at odds with the expectation that T Tauri stars are formed by the gravitational collapse of rotating molecular cores and the presence of disks surrounding the stars. Theories which explain the slow rotations generally invoke the interaction between the disk and the stellar magnetic field of a few kG (e.g., Königl 1991; Cameron & Campbell 1993; Shu et al. 1994; Yi 1995; Armitage & Clarke 1996). Since the growth time for disk warping is short, we may expect the inner disk of T Tauri stars to wander around the “preferred” perpendicular state. The star therefore experiences both spin-up and spin-down during its evolution, analogous to the behavior of X-ray pulsars (see §6.1). The net, secular spin-up rate is expected to be much smaller than that based on the canonical spin-up torque ( $\sim \dot{M} \sqrt{GM r_m}$ ).

## 7. CONCLUSION

In this paper we have identified a new magnetically driven warping instability which occurs in the inner accretion disk of a magnetized star (§2 and §4). Despite the uncertainties in our understanding of the magnetosphere–disk interactions (particularly the global magnetic field structure), the existence of the instability seems robust, and requires that some vertical field lines

(either from the star or intrinsic to the disk) thread the disk and get twisted by the disk rotation. The general consequence of the instability is that the normal vector of the inner disk (near the magnetosphere) will be tilted with respect to the stellar spin axis. We have also shown that the disk can be driven magnetically into precession around the spin axis due to the interaction between the screening surface current and the stellar magnetic field (§2). In addition, certain regions of the disk are subjected to resonant magnetic forces which may affect the structure and dynamics of the disk (§3). These magnetic effects on accretion disks have largely been overlooked in previous studies of accretion onto magnetic stars <sup>17</sup>.

We have applied our theory to several different types of astrophysical systems, including X-ray pulsars, low-mass X-ray binaries, and T Tauri stars (§6). These applications should be considered preliminary, but they indicate that the magnetically driven disk warping and precession can potentially play an important role in determining the observational behaviors of these systems. Of particular interest is that the magnetically warped inner disk may provide a natural explanation for the longstanding puzzle of torque reversal as observed in a number of X-ray pulsars. Also, the tilted disk may be responsible for the rich phenomenology of time variability (such as QPOs) observed in weakly magnetized accreting neutron stars in LMXBs.

Much work is needed to understand better the effects studied in this paper and their observational manifestations in different astrophysical systems. In our analysis, we have intentionally avoided (or bypassed), by using parametrized models, the uncertainties associated with magnetosphere – disk interactions (see, e.g., Appendix A,B), but clearly the study of disk warping and precession based on more specific models (with or without outflows) would be useful. The role of intrinsic disk field needs to be examined further (see §2.4). There remains uncertainty in the description of nonlinear warped disks, and a full numerical simulation of the nonlinear development of the warping instability would be valuable. In the case of low-mass X-ray binaries, the effects of complex magnetic field topology (other than dipole) and general relativity should be included to access the QPO phenomenology (see §6.2). More detailed comparison with observational data will be useful. The role of magnetically driven resonances need to be studied further to determine whether they will produce any observable features. We hope to address some of these issues in the future.

I thank Richard Lovelace, Phil Maloney, Dimitrios Psaltis, Marten van Kerkwijk and Ethan Vishniac for useful discussion/comment. I also thank Brad Hansen for informing me of some important references. I became puzzled by the spin-up/spin-down behavior of X-ray pulsars several years ago at Caltech through discussions with Lars Bildsten, Deepto Chakrabarty, Rob Nelson and Tom Prince. I acknowledge the support from a NASA ATP grant and a research

---

<sup>17</sup>We note that the effects studied in this paper are quite different from the situation considered by Agapitou et al. (1997), who studied the bending instability in the inner (sub-Keplerian) disk which corotates with the star (with the magnetic axis aligned with the spin axis). Such a disk may or may not exist (see Spruit & Taam 1990).

fellowship from the Alfred P. Sloan foundation, as well as support from Cornell University.

### A. MAGNETIZED ACCRETION DISK

For an accretion disk threaded by a vertical magnetic field  $B_z$ , the steady-state angular momentum equation reads:

$$V_r \frac{dl}{dr} = \frac{r}{\Sigma} \left[ \frac{1}{r^2} \frac{d}{dr} \left( r^3 \Sigma \nu_1 \frac{d\Omega}{dr} \right) + \frac{B_z \Delta B_\phi}{2\pi} \right], \quad (\text{A1})$$

where  $l$  is the angular momentum per unit mass,  $\Sigma$  is the surface density,  $\Delta B_\phi$  is the  $\phi$ -component of the magnetic field produced by twisting  $B_z$  and evaluated at the upper disk surface. Integrating over  $r$  and using the mass continuity equation  $\dot{M} = -2\pi r \Sigma V_r$ , we obtain the conservation equation for angular momentum:

$$\dot{M} l_0 = \dot{M} l + 2\pi \nu_1 r^3 \Sigma \Omega' + \dot{M} l_B, \quad (\text{A2})$$

where  $l_0$  is a constant,  $\Omega' \equiv d\Omega/dr$ , and

$$\dot{M} l_B = - \int_r^\infty dr r^2 B_z \Delta B_\phi. \quad (\text{A3})$$

Equation (A2) says that the rate of net angular momentum transfer through the disk,  $\dot{M} l_0$ , is equal to the sum of the rates of advective, viscous, and magnetic transport. We can rewrite (A2) as

$$\Sigma = - \frac{\dot{M} \Omega}{2\pi r \nu_1 \Omega'} \mathcal{J}, \quad (\text{A4})$$

where

$$\mathcal{J} \equiv 1 - \frac{l_0 - l_B}{l}. \quad (\text{A5})$$

The radial velocity is

$$V_r = \frac{\nu_1 \Omega'}{\Omega} \mathcal{J}^{-1}. \quad (\text{A6})$$

For a Keplerian flow,  $\Omega = \sqrt{GM/r^3}$ ,  $l = \sqrt{GM}r$ , and eqs. (A4)-(A6) reduce to (4-2). The standard thin disk equations are recovered if we set  $l_B = 0$ .

The above equations are quite general, but the actual expression for  $l_B$  depends on the behavior of the disk magnetic field, and thus should be viewed as being uncertain. Consider a specific ansatz:

$$B_z = B_0 \left( \frac{R}{r} \right)^3, \quad \Delta B_\phi = -\zeta B_z \quad (\text{A7})$$

(see eqs. [2-27]-[2-28]), where  $B_0$  measures the magnetic field at the stellar surface ( $r = R$ ).

Assuming that  $\zeta$  is a constant, we find

$$l_B = \frac{\zeta B_0^2}{3\dot{M}r^3} = \frac{1}{3} b^2 l_R \left( \frac{R}{r} \right)^3, \quad (\text{A8})$$

where  $l_R \equiv \sqrt{GM R}$  and  $b^2 \equiv \zeta B_0^2 R^3 / (\dot{M} l_R)$  is dimensionless. More general expressions (including spin dependence, multipole field and general relativistic effect) can be found in Lai (1998). The inner edge of the disk,  $r_m$ , can be formally defined as where where  $d(l + l_B)/dr = 0$ ; we find

$$r_m = R (2b^2)^{2/7} = \left( \frac{2\zeta B_0^2 R^6}{\dot{M} \sqrt{GM}} \right)^{2/7} \quad (\text{A9})$$

(cf. eq. [1-1]). We then have

$$l_0 = l(r_m) + l_B(r_m) = \frac{7}{6} l(r_m) = \frac{7}{6} \sqrt{GM r_m}, \quad (\text{A10})$$

and

$$\mathcal{J} = 1 - \frac{1}{6} \left( \frac{r_m}{r} \right)^{1/2} \left[ 7 - \left( \frac{r_m}{r} \right)^3 \right]. \quad (\text{A11})$$

This would suggest  $\mathcal{J} = 0$  at  $r = r_m$ . But of course as  $r$  approaches the inner disk boundary, this expression breaks down, as the inertial term of the radial equation must be taken into account (see Lai 1998 for a magnetic slim disk model).

## B. MAGNETOSPHERE RADIUS FOR GENERAL FIELD GEOMETRY

In the main text, we have intentionally avoided the precise definition of the magnetosphere radius  $r_m$  for general orientations of  $\hat{l}$ ,  $\hat{\omega}$  and  $\hat{\mu}$ . This is because the exact determination of  $r_m$  requires a detailed model of the structure of magnetosphere–disk boundary layer, for which no definitive theory exists (useful discussions are contained in the references cited in §1). We offer the following three possibilities. They should be viewed only as an educated guess, although they all give a scaling relation as in eq. (1-1).

(i) *Ansatz 1*: If the static vertical field  $B_z = -(\mu/r^3) \cos \beta \cos \theta$  threads the disk (see §2.3), it will affect the angular momentum transport in the disk through the magnetic stress  $\propto B_z \Delta B_\phi$ , where  $B_\phi = -\zeta B_z$  is the field created by winding  $B_z$  (see eqs. [A2]-[A3]). When the condition

$$\dot{M} \frac{dl}{dr} + r^2 B_z \Delta B_\phi = 0 \quad (\text{B1})$$

(where  $l = \sqrt{GM r}$  is the angular momentum per unit mass) is satisfied, no viscosity is needed to induce accretion. We may thus use this condition to determine the inner edge of the Keplerian disk, giving

$$r_m = \left( 2\zeta \cos^2 \beta \cos^2 \theta \right)^{2/7} \left( \frac{\mu^4}{GM \dot{M}^2} \right)^{1/7}. \quad (\text{B2})$$

(ii) *Ansatz 2*: Here we shall follow the consideration similar to that in Arons (1993). Assume that the disk is largely diamagnetic, but strong dissipation exists at the boundary layer, where

plasma stress and magnetic stress balance, i.e.,

$$\rho V_r V_\phi = \frac{B_z \Delta B_\phi}{4\pi}. \quad (\text{B3})$$

The vertical magnetic field at the disk inner edge ( $r = r_m$ ) is given by

$$B_z(r_m) = -\frac{4\mu}{\pi r_m^3} \left(\frac{r_m}{2H}\right)^{1/2} \cos \chi \quad (\text{B4})$$

(Aly 1980). Shear in the boundary layer induces  $\Delta B_\phi = -\zeta_B B_z$  with  $\zeta_B \lesssim 1$ . Using  $V_\phi = \sqrt{GM/r}$  and  $V_r = -\dot{M}/(4\pi r \rho H)$ , we find

$$r_m = \left(\frac{8\zeta_B}{\pi^2} \cos^2 \chi\right)^{2/7} \left(\frac{\mu^4}{GMM^2}\right)^{1/7}. \quad (\text{B5})$$

Since  $\cos \chi = \cos \beta \cos \theta - \sin \beta \sin \theta \sin \omega t$ , eq. (B5) implies that the magnetosphere boundary is modulated at the spin frequency  $\omega$ . If we average the magnetic stress over time, we may replace  $\cos^2 \chi$  by  $[\cos^2 \beta \cos^2 \theta + (1/2) \sin^2 \beta \sin^2 \theta]$ .

(iii) *Ansatz 3*: This is similar to (ii), except that we now assume that the static vertical field threads the disk [see eq. (2-25)], so that at  $r = r_m$ ,

$$B_z(r_m) = -\frac{\mu}{r_m^3} \cos \beta \cos \theta + \frac{4\mu}{\pi r_m^3} \left(\frac{r_m}{2H}\right)^{1/2} \sin \beta \sin \theta \sin \omega t. \quad (\text{B6})$$

The condition (B3) then gives

$$r_m = \left(\frac{8\zeta_B}{\pi^2}\right)^{2/7} \left[ \sin \beta \sin \theta \sin \omega t - \frac{\pi}{4} \left(\frac{2H}{r_m}\right)^{1/2} \cos \beta \cos \theta \right]^{4/7} \left(\frac{\mu^4}{GMM^2}\right)^{1/7}. \quad (\text{B7})$$

We see that in general, the inclined rotating dipole will produce a time-varying magnetosphere boundary. This variability may be in addition to that associated the winding-up and reconnection of field lines (see the end of §2.4).

### C. MOTION OF DIAMAGNETIC BLOBS

It has recently been suggested that under certain conditions, the accretion disk onto magnetized object may consist of diamagnetic blobs (King 1993; Vietri & Stella 1998). Here we study how the stellar magnetic field affects the motion of diamagnetic blobs which lie in circular orbits of the disk plane. Each blob moves independent of each other, and is subjected to the gravitational force from the central star and the magnetic drag force which arises when it moves across the field lines (see below). It is not clear that a realistic disk will behave as a collection of individual blobs, nor is it clear that the blob can survive for a long time (e.g., the blobs may be

subjected further Kelvin-Helmholtz instability which tends to break up the blobs) — These issues are not addressed in this paper. Our purpose here is to understand the dynamics of the blob under the afore-mentioned assumptions.

Vietri and Stella (1998) has studied some aspects of this problem. They assumed that the spin axis is aligned with the angular momentum axis of the orbiting blob. They showed that vertical resonances exist in the region where  $\omega/2 \leq \Omega \leq 3\omega/2$  (where  $\omega$ ,  $\Omega$  are the spin frequency and orbital frequency), and suggested that the resonances can pump the blobs out of the equatorial plane. Here we consider the more general case where the orbital angular momentum of the blob is misaligned with the spin axis. We show that even without the resonances, there exists a magnetic torque which can induce tilt of the orbit of the blob.

Our setup is given in Fig. 1. The magnetic drag force on the blob results from the Lorentz force on the screening current on the blob’s surface. The blob loses energy by exciting Alfvén waves in the surrounding plasma. The drag force per unit mass is given by

$$\mathbf{F}_{\text{drag}} = -\frac{\Delta\mathbf{V}_{\perp}}{\tau_d}, \quad (\text{C1})$$

and the drag time scale is

$$\tau_d = \frac{c_A m}{B^2 d^2}. \quad (\text{C2})$$

Here  $c_A$  is the Alfvén speed in the interblob plasma (where the field strength is  $B$ ), and  $m$  and  $d$  is the mass and characteristic size of the blob (Drell, Foley & Ruderman 1965). We shall assume that the interblob field is that of the stellar dipole (thus neglecting possible screening due to the blobs):

$$B_r = \frac{2\mu}{r^3} \sin \chi \cos(\phi - \phi_\mu), \quad (\text{C3})$$

$$B_\phi = \frac{\mu}{r^3} \sin \chi \sin(\phi - \phi_\mu), \quad (\text{C4})$$

$$B_z = -\frac{\mu}{r^3} \cos \chi. \quad (\text{C5})$$

The relative velocity between the blob and the field line [at location  $(r, \phi, z = 0)$ ] is

$$\Delta\mathbf{V} = \Omega r \hat{\phi} - \Omega_s \hat{\omega} \times \mathbf{r}. \quad (\text{C6})$$

The projected relative velocity perpendicular to the field line is then

$$\begin{aligned} \Delta\mathbf{V}_{\perp} &= \Delta\mathbf{V} - \frac{(\mathbf{B} \cdot \Delta\mathbf{V}) \mathbf{B}}{|\mathbf{B}|^2} \\ &= \Delta\Omega r \hat{\phi} + \omega r \sin \beta \cos \phi \hat{z} \\ &\quad - \frac{r}{C} \left[ \Delta\Omega \sin \chi \sin(\phi - \phi_\mu) - \omega \cos \chi \sin \beta \cos \phi \right] \\ &\quad \times \left[ 2 \sin \chi \cos(\phi - \phi_\mu) \hat{r} + \sin \chi \sin(\phi - \phi_\mu) \hat{\phi} - \cos \chi \hat{z} \right], \end{aligned} \quad (\text{C7})$$

where

$$C \equiv 1 + 3 \sin^2 \chi \cos^2(\phi - \phi_\mu), \quad (\text{C8})$$

$$\Delta\Omega \equiv \Omega - \omega \cos \beta. \quad (\text{C9})$$

The drag constant can be written as

$$\tau_d^{-1} = \frac{d^2 \mu^2}{m c_A r^6} C = \tau_{d0}^{-1} C^{1/2}, \quad (\text{C10})$$

where

$$\tau_{d0}^{-1} = \frac{d^2 \mu}{m r^3} (4\pi \rho_0)^{1/2}, \quad (\text{C11})$$

( $\rho_0$  is the density of the interblob medium). The second equality of eq. (C10) is valid only when  $c_A$  is less than the speed of light.

### C.1. Magnetic Torques

The magnetic torque on the blob (per unit mass) is given by

$$\begin{aligned} \mathbf{N} &= -\frac{r}{\tau_{d0}} C^{1/2} \hat{r} \times \Delta \mathbf{V}_\perp \\ &= -\frac{r^2}{\tau_{d0}} \left\{ C^{1/2} \left( \Delta\Omega \hat{z} - \omega \sin \beta \cos \phi \hat{\phi} \right) \right. \\ &\quad \left. - C^{-1/2} \left[ \Delta\Omega \sin \chi \sin(\phi - \phi_\mu) - \omega \cos \chi \sin \beta \cos \phi \right] \right. \\ &\quad \left. \times \left[ \sin \chi \sin(\phi - \phi_\mu) \hat{z} + \cos \chi \hat{\phi} \right] \right\}. \end{aligned} \quad (\text{C12})$$

To average over  $\phi$ , we shall approximate  $C^{1/2}$  by  $C_1^{1/2}$  and  $C^{-1/2}$  by  $C_2^{-1/2}$ , where  $C_1$  and  $C_2$  are constants in the range of 1–4. Since the Taylor expansion of  $C^{1/2}$  or  $C^{-1/2}$  contains  $\cos 2n(\phi - \phi_\mu)$  (where  $n$  is an integer), we can be sure that no new term (with different dependence on the angles) would appear if the exact expression of  $C^{1/2}$  or  $C^{-1/2}$  were adopted. We find

$$\begin{aligned} \langle \mathbf{N} \rangle_\phi &= -\frac{r^2}{\tau_{d0}} C_1^{1/2} \left( \Delta\Omega \hat{z} - \frac{1}{2} \omega \sin \beta \hat{y} \right) - \frac{r^2}{2\tau_{d0}} C_2^{-1/2} \left[ \Delta\Omega \sin \chi \cos \chi \cos \phi_\mu \hat{x} \right. \\ &\quad \left. + \left( \Delta\Omega \sin \chi \cos \chi \sin \phi_\mu + \omega \sin \beta \cos^2 \chi \right) \hat{y} \right. \\ &\quad \left. - \left( \Delta\Omega \sin^2 \chi + \omega \sin \beta \sin \chi \cos \chi \sin \phi_\mu \right) \hat{z} \right]. \end{aligned} \quad (\text{C13})$$

Averaging over the rotation period and using the identities (2-9)-(2-11) we obtain

$$\langle \langle \mathbf{N} \rangle \rangle = -\frac{r^2}{\tau_{d0}} C_1^{1/2} \left( \Delta\Omega \hat{z} - \frac{1}{2} \omega \sin \beta \hat{y} \right)$$



$$\begin{aligned}
& -\frac{r^2}{2\tau_{d0}}C_2^{-1/2}\left\{\left[\omega\cos^2\theta+\frac{1}{2}(\Omega\cos\beta-\omega)(3\cos^2\theta-1)\right]\sin\beta\hat{y}\right. \\
& \left.-\left[\Delta\Omega\sin^2\theta+\frac{1}{2}\Omega\sin^2\beta(3\cos^2\theta-1)\right]\hat{z}\right\}. \tag{C14}
\end{aligned}$$

In the case of  $\beta = 0$  (i.e., aligned  $\hat{\omega}$  and  $\hat{l}$ ), the only nonzero torque is along the  $z$ -axis:

$$\langle\langle\mathbf{N}\rangle\rangle = -\frac{r^2}{\tau_{d0}}\left(C_1^{1/2}-\frac{1}{2}C_2^{-1/2}\sin^2\theta\right)(\Omega-\omega)\hat{z}, \quad (\beta=0). \tag{C15}$$

This is simply the magnetic braking torque which tends to drive the blob toward corotation with the magnetic field lines. For  $\beta \neq 0$ , there is another torque in the  $y$ -direction, which tends to tilt the orbit of the blob. In the absence of other forces, the tilt angle  $\beta$  evolves according to

$$\frac{d\beta}{dt} = \frac{1}{4\tau_{d0}}\sin\beta\left[C_2^{-1/2}(3\cos^2\theta-1)\cos\beta+\frac{\omega}{\Omega}(C_2^{-1/2}\sin^2\theta-2C_1^{1/2})\right]. \tag{C16}$$

When  $\omega \ll \Omega$ , this equation has a similar structure as eq. (2-22). Clearly, under certain conditions (when the quantity inside the square bracket is positive), there is an instability where  $\beta$  tends to grow toward the perpendicular state ( $\beta = 90^\circ$ ). The growth time is of order  $\tau_{d0}$ .

## C.2. Resonances

The vertical magnetic force (per unit mass) on the blob is given by

$$\begin{aligned}
F_z &= -\tau_{d0}^{-1}C^{1/2}\omega r\sin\beta\cos\phi \\
& -\tau_{d0}^{-1}C^{-1/2}r\cos\chi\left[\Delta\Omega\sin\chi\sin(\phi-\phi_\mu)-\omega\cos\chi\sin\beta\cos\phi\right]. \tag{C17}
\end{aligned}$$

The equation of motion for the vertical motion is simply

$$\frac{d^2Z}{dt^2} + \Omega_z^2 Z = F_z. \tag{C18}$$

First consider the case where  $\beta = 0$ . The time-dependence of the force is as in  $C^{-1/2}\sin(\phi - \omega t)$ , which can be written as a sum of  $\sin(2n + 1)(\phi - \omega t)$ . Thus the resonance conditions are  $(2n + 1)(\omega - \Omega) = \pm\Omega_z$ , or, for  $\Omega_z = \Omega$  (Keplerian disk):

$$\omega = \frac{2n}{2n+1}\Omega, \quad \text{or} \quad \omega = \frac{2n+2}{2n+1}\Omega, \quad (n = 0, 1, 2, \dots). \tag{C19}$$

Thus the resonance “band” lies in  $\omega/2 \leq \Omega \leq 3\omega/2$  (but excluding  $\omega = \Omega$ ). This was first identified by Vietri & Stella (1998). Note that for  $\omega = 0$ , the resonance  $\Omega_z = \Omega$  is always satisfied, which implies that the blob will be driven out of the equatorial plane.

Now for the general  $\beta \neq 0$  cases. If we treat  $C$  as being independent of time, then it is easy to identify the following resonances: (i)  $\Omega_z = \Omega$  (which is always satisfied for a Keplerian disk); (ii)  $\omega \pm \Omega = \pm\Omega_z$ ; (iii)  $2\omega \pm \Omega = \pm\Omega_z$ . To take account of the time-dependence of  $C$ , we note that

$$C = 1 + 3 \left[ \sin \theta \sin^2 \frac{\beta}{2} \cos(\phi + \omega t) + \sin \theta \cos^2 \frac{\beta}{2} \cos(\phi - \omega t) + \cos \theta \sin \beta \sin \phi \right]^2. \quad (\text{C20})$$

Thus  $C^{1/2}$  or  $C^{-1/2}$  can be written as a sum of  $\cos(2n\phi \pm m\omega t)$  and  $\sin(2n\phi \pm m\omega t)$  (where  $n, m = 0, 1, 2, \dots$ ). We can then show that resonances occur when  $2n\Omega = m\omega$  (for  $\Omega_z = \Omega$ ), i.e., all blobs (with different orbital radii) are subjected to resonant forcing. We expect that the high-order resonances (those with large  $n$  and  $m$ ) are weak, although we have not tried to quantify them. The ubiquity of the vertical resonances implies that the disk consisting of diamagnetic blobs tends to thicken due to the magnetic drag force.

The radial force (per unit mass) on the blob is given by

$$F_r = 2\tau_{d0}^{-1} C^{-1/2} r \sin \chi \cos(\phi - \phi_\mu) \left[ \Delta\Omega \sin \chi \sin(\phi - \phi_\mu) - \omega \cos \chi \sin \beta \cos \phi \right]. \quad (\text{C21})$$

Similar consideration reveals the existence of a large number of epicyclic resonances in the disk.

## REFERENCES

- Agapitou, V., Papaloizou, J. C. B., & Terquem, C. 1997, MNRAS, 292, 631.
- Alpar, A., Cheng, A. F., Ruderman, M., & Shaham, J. 1982, Nature, 300, 728.
- Alpar, M. A., & Shaham, J. 1985, Nature, 316, 239.
- Aly, J. J. 1980, A&A, 86, 192.
- Aly, J. J., & Kuijpers, J. 1990, A&A, 227, 473.
- Anzer, U., & Börner, G. 1980, A&A, 83, 133.
- Anzer, U., & Börner, G. 1983, A&A, 122, 73.
- Armitage, P. J., & Clarke, C. J. 1996, MNRAS, 280, 458.
- Arons, J. 1987, in “The Origin and Evolution of Neutron Stars” (IAU Symp. No. 125), ed. D. J. Helfand & J.-H. Huang (D. Reidel Pub.: Dordrecht).
- Arons, J. 1993, ApJ, 408, 160.
- Arons, J., & Lea, S. M. 1980, ApJ, 235, 1016.
- Bardeen, J. M., & Petterson, J. A. 1975, ApJ, 195, L65.

- Basri, G, Marcy, G. W., & Valenti, J. A. 1992, *ApJ*, 390, 622.
- Bertout, C. 1989, *ARA&A*, 27, 375.
- Bhattacharya, D. 1995, in “X-ray Binaries”, ed. W.H.G. Lewin, J. van Paradijs & E.P.J. van den Heuvel (Cambridge Univ. Press).
- Bildsten, L., et al. 1997, *ApJS*, 113, 367.
- Blandford, R. D. 1989, in *Theory of Accretion Disks*, ed. F. Meyer et al. (Kluwer Academic Pub.: Dordrecht).
- Bouvier, J., et al. 1995, *A&A*, 299, 89.
- Burns, J. A., Schaffer, L. E., Greenberg, R. J., & Showalter, M. R. 1985, *Nature*, 316, 115.
- Cameron, A. C., & Campbell, C. G. 1993, *A&A*, 274, 309.
- Campbell, C. G. 1997, *Magnetohydrodynamics in Binary Stars* (Kluwer Academic Pub.: Dordrecht).
- Chakrabarty, D., et al. 1997, *ApJ*, 481, L101.
- Deeter, J. E., et al. 1998, *ApJ*, 502, 802.
- Drell, S. D., Foley, H. M., & Ruderman, M. A. 1965, *J. Geophys. Res.*, 70, 3131.
- Ford, E. C., & van der Klis, M. 1998, 506, L39.
- Frank, J., King, A., & Raine, D. 1992, *Accretion Power in Astrophysics* (Cambridge Univ. Press).
- Ghosh, P., & Lamb, F. K. 1979a, *ApJ*, 232, 259.
- Ghosh, P., & Lamb, F. K. 1979b, *ApJ*, 234, 296.
- Ghosh, P., & Lamb, F. K. 1992, in *X-ray Binaries and Recycled Pulsars*, ed. E.P.J. van den Heuvel and S.A. Rappaport (Dordrecht: Kluwer).
- Goodson, A. P., Winglee, R. M., & Böhm, K.-H. 1997, *ApJ*, 489, 199.
- Hartmann, L. 1998, *Accretion Processes in Star Formation* (Cambridge Univ. Press).
- Hasinger, G., & van der Klis, M. 1989, *A&A*, 225, 79.
- Hayashi, M. R., Shibata, K., & Matsumoto, R. 1996, *ApJ*, 468, L37.
- Ipsier, J. R. 1996, *ApJ*, 458, 508.
- Katz, J. I. 1973, *Nature Phys. Sci.*, 246, 87.

- King, A. R. 1993, MNRAS, 261, 144.
- Königl, A. 1991, ApJ, 370, L39.
- Kumar, S., & Pringle, J. E. 1992, MNRAS, 258, 811.
- Kundt, W., & Robnik, M. 1980, A&A, 91, 305.
- Lai, D. 1998, ApJ, 502, 721.
- Lai, D., Lovelace, R. V. E., & Wasserman, I. 1999, submitted to ApJ (astro-ph/9904111).
- Lamb, F. K., Pethick, C. J., & Pines, D. 1973, ApJ, 184, 271.
- Lamb, F. K., Shibazaki, N., Alpar, M. A., & Shaham, J. 1985, Nature, 317, 681.
- Lang, F. L., et al. 1981, ApJ, 246, L21.
- Li, J., Wickramasinge, D. T., & Rüdiger, G. 1996, ApJ, 469, 765.
- Lipunov, V. M., Semënov, E. S., & Shakura, N. I. 1981, Sov. Astron., 25, 439.
- Lipunov, V. M., & Shakura, N. I. 1980, Sov. Astron. Lett., 6, 14.
- Lovelace, R. V. E., Romanova, M. M., & Bisnovatyi-Kogan, G. S. 1995, MNRAS, 275, 244.
- Lovelace, R. V. E., Romanova, M. M., & Bisnovatyi-Kogan, G. S. 1998, ApJ, in press (astro-ph/9811369).
- Lynden-Bell, D., & Boily, C. 1994, MNRAS, 267, 146.
- Maloney, P. R., & Begelman, M. C. 1997, ApJ, 491, L43.
- Margon, B. 1984, ARA&A, 22, 507.
- Marković, D., & Lamb, F. K. 1998, ApJ, 507, 316.
- Méndez, M., et al. 1998a, ApJ, 494, L65.
- Méndez, M., van der Klis, M., & van Paradijs, J. 1998b, ApJ, 505, L23.
- Miller, M. C., Lamb, F. K., & Psaltis, D. 1998, ApJ, 508, 791.
- Miller, K. A., & Stone, J. M. 1997, ApJ, 489, 890.
- Morsink, S. M., & Stella, L. 1999, ApJ, 513, 827.
- Nelson, R. W., et al. 1997, ApJ, 488, L117.
- Newman, W. I., Newman, A. L., & Lovelace, R. V. E. 1992, ApJ, 392, 622.

- Novikov, I. D., & Thorne, K. S. 1973, in *Black Holes*, ed. C. DeWitt and B. DeWitt (Gordon and Breach: New York).
- Ogilvie, G. I. 1999, *MNRAS*, 304, 557.
- Papaloizou, J. C., & Pringle, J. E. 1983, *MNRAS*, 202, 1181.
- Park, S. J., & Vishniac, E. T. 1996, *ApJ*, 471, 158.
- Phinney, E. S., & Kulkarni, S. R. 1994, *ARA&A*, 32, 591.
- Priedhorsky, W. C., & Holt, S. S. 1987, *Space Sci. Rev.*, 45, 291.
- Pringle, J. E. 1992, *MNRAS*, 258, 811.
- Pringle, J. E. 1996, *MNRAS*, 281, 857.
- Pringle, J. E., & Rees, M. J. 1972, *A&A*, 21, 1.
- Psaltis, D., et al. 1999, submitted to *ApJ*.
- Riffert, H. 1980, *Astro. Space. Sci.*, 71, 195.
- Schaffer, L., & Burns, J. A. 1992, *ICARUS*, 96, 65.
- Shakura, N. I., & Sunyaev, R. A. 1973, *A&A*, 24, 337.
- Sheffer, E. K., et al. 1992, *Sov. Astron.*, 36, 41.
- Shu, F. H., et al. 1994, *ApJ*, 429, 781.
- Spruit, H. C., & Taam, R. E. 1990, *A&A*, 229, 475.
- Spruit, H. C., & Taam, R. E. 1993, *ApJ*, 402, 593.
- Scheuer, P. A. G., & Feiler, R. 1996, *MNRAS*, 282, 291.
- Stella, L., & Vietri, M. 1998, *ApJ*, 492, L59.
- Stella, L., & Vietri, M. 1999, *Phys. Rev. Lett.*, in press (astro-ph/9812124).
- Stone, J. M., & Norman, M. L. 1994, *ApJ*, 433, 746.
- Sturrock, P. A., & Barnes, C. 1972, *ApJ*, 176, 31.
- Tananbaum, H., et al. 1972, *ApJ*, 174, L143.
- Torkelsson, U. 1998, astro-ph/9803068.
- Toropin, Y. M., et al. 1999, *ApJ*, in press.

- van Ballegoijen, A. A. 1994, *Space Science Rev.*, 68, 299.
- Van der Klis, M. 1995, in “X-ray Binaries”, ed. W.H.G. Lewin, J. van Paradijs & E.P.J. van den Heuvel (Cambridge Univ. Press).
- Van der Klis, M. 1998a, in “The Many Faces of Neutron Stars” (Proc. NATO ASI) (astro-ph/9710016).
- Van der Klis, M. 1998b, astro-ph/9812395.
- Van der Klis, M., et al. 1985, *Nature*, 316, 225.
- Van der Klis, M., Wijnands, R. A., Horne, K., & Chen, W. 1997, *ApJ*, 481, L97.
- Van Kerkwijk, M. H., et al. 1998, *ApJ*, 499, L27.
- Vietri, M., & Stella, L. 1998, *ApJ*, 503, 350.
- Wang, Y.-M. 1987, *A&A*, 183, 257.
- Wang, Y.-M. 1995, *ApJ*, 449, L153.
- Wijers, R. A. M. J., & Pringle, J. E. 1998, astro-ph/9811056.
- Yi, I. 1995, *ApJ*, 442, 768.
- Yi, I., & Kenyon, S. J. 1997, *ApJ*, 477, 379.
- Yi, I., Wheeler, C., & Vishniac, E. T. 1997, *ApJ*, 481, L51.

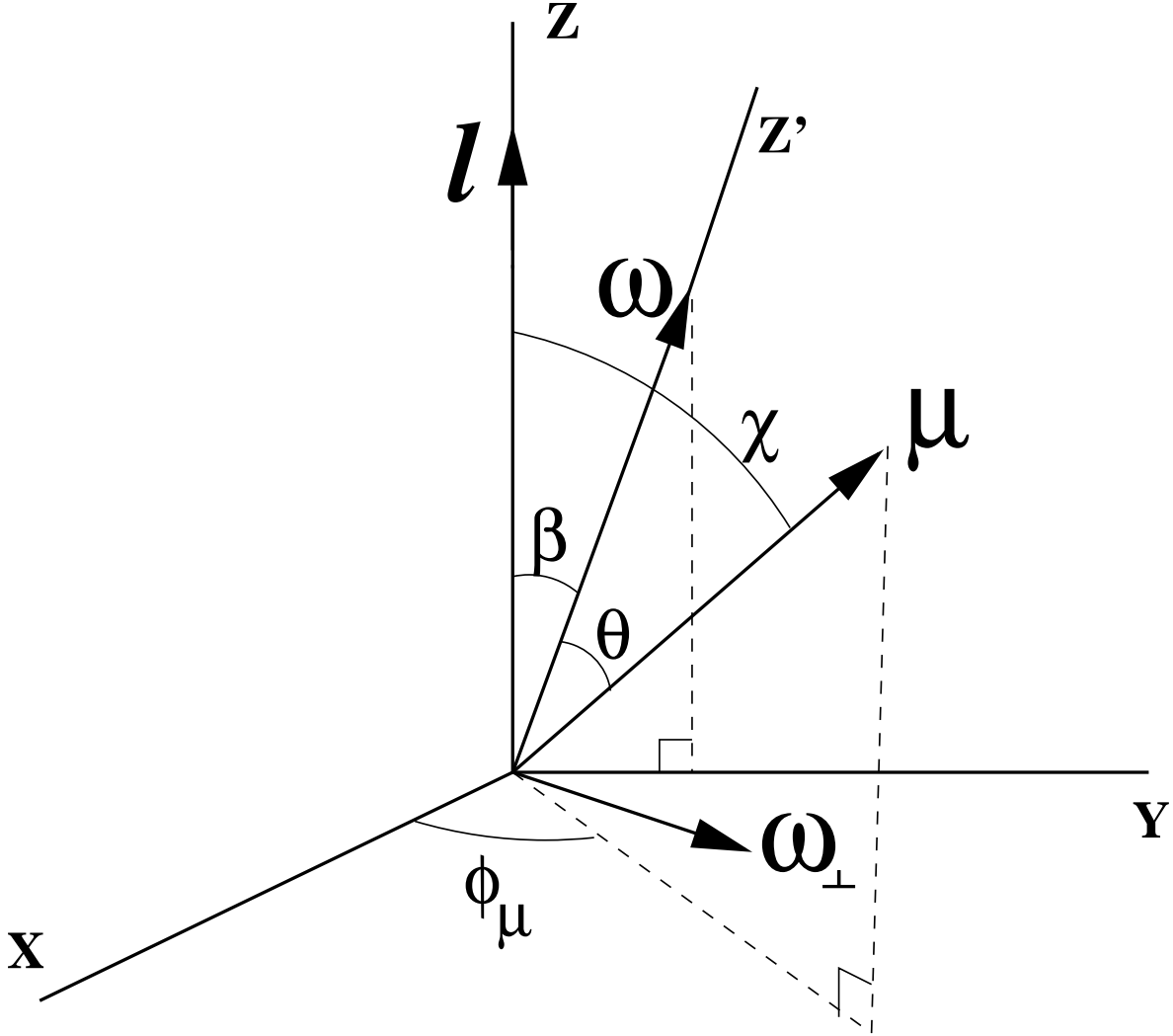


Fig. 1.— Coordinate system used in the calculation. The  $z$ -axis is along  $l$ , the angular momentum of the disk (or a ring of disk). The angular velocity vector of the star,  $\omega = \omega \hat{\omega}$  (where  $\hat{\omega}$  is the unit vector) is inclined at an angle  $\beta$  with respect to  $l$ , and lies in the  $yz$ -plane. The stellar dipole moment  $\mu = \mu \hat{\mu}$  (where  $\hat{\mu}$  is the unit vector) rotates around  $\hat{\omega}$ , and the angle of obliquity is  $\theta$ . In the cartesian coordinate, we have  $\hat{\mu} = \sin \chi \cos \phi_{\mu} \hat{x} + \sin \chi \sin \phi_{\mu} \hat{y} + \cos \chi \hat{z}$ . The axis  $z'$  (along the spin axis) is used for studying disk warping, and  $\omega_{\perp}$  is the unit vector perpendicular to  $\omega$  and lies in the  $yz$ -plane.